Carbohydrate Research, 243 (1993) 225–258
Elsevier Science Publishers B.V., Amsterdam

Influence of sulfate and carboxylate groups on the conformation of chondroitin sulfate related disaccharides

Marianne Zsiška and Bernd Meyer *

Complex Carbohydrate Research Center and Departments of Biochemistry and Chemistry, University of Georgia, Athens, GA 30602 (USA)

(Received October 12th, 1992; accepted with revisions December 7th, 1992)

ABSTRACT

^{1}H NMR and ^{13}C NMR spectral parameters of eight sulfated uronic acid containing disaccharides **1–8** were used to determine the conformational preferences that depend on the pattern of sulfation. Three sulfated derivatives of benzyl β-D-Gal-(1 → 4)-β-D-GlcA (**1**), its 6′-sulfate **2**, 4′-sulfate **3**, and 4′,6′-disulfate **4** were used as models for the β-(1 → 4) glycosidic linkage of chondroitin sulfates and three sulfated derivatives of benzyl β-D-GlcA-(1 → 3)-β-D-Gal (**5**), its 6-sulfate **6**, 4-sulfate **7**, and 4,6-disulfate **8** were used as models for the β-(1 → 3) glycosidic linkage of chondroitin sulfates. To determine the dependence of conformational preferences on the charged groups, the sulfated disaccharides **2**, **3**, and **4** were compared to their unsulfated parent compound **1**, and **6**, **7**, and **8** were compared to their parent compound **5**. The $^3J_{H\text{-}5,H\text{-}6}$ coupling constants were determined by high-order analysis of the spin systems, and from these the preferred populations of the hydroxymethyl groups were calculated. Selective 1D NOEs and ROEs were measured from H-1′ across the glycosidic linkage to obtain the average distance of the protons adjacent to the glycosidic linkage. Derivatives of β-D-Gal-(1 → 4)-β-D-GlcA carrying a sulfate group in the 6′-position (**2**) and in the 4′- and 6′-position (**4**) show a slight repulsive effect between the 6′-sulfate groups and the carboxylate group as expressed in small changes of the preferred populations of the glycosidic linkage and the sulfonyloxymethyl group. The 4-sulfate groups in **3** and **4** do not show a significant influence on the glycosidic linkage. However, the two sulfate groups in **4** exhibit a repulsive effect leading to a very high population of the *gt* conformation of the sulfonyloxymethyl group. In contrast hereto, the sulfate group at C-4 of β-D-GlcA-(1 → 3)-β-D-Gal disaccharides **7** and **8** and the carboxylate group exert an attractive interaction that leads to a change of the conformation of the glycosidic linkage in **7** and **8** by about 30°. The 6-sulfate groups of the disaccharides **6** and **8** show a slight repulsive interaction with the carboxylate and/or 4-sulfate group. Changes in ^{13}C NMR chemical shifts support the interpretation obtained from the NOE and ROE analysis. Relative NOE ratios were used to estimate the correlation time to $\tau_c = 3.5\text{–}4.0 \times 10^{-10}$ s for **1–8**, and these were found to be in agreement with calculated T_1 values. The charge–charge interaction energies observed are fairly small in **1–8**. The largest effect can be observed in the rotamer population of the C-6 groups of the disulfates **4** and **8**, which leads to an effective interaction energy of the two sulfate groups of ≈ 1.0 kcal/mol. This is equivalent to an effective dielectric constant of $\epsilon \approx 10$, assuming that full charges are expressed on the sulfate groups. Ensemble average values for observable ϵ of **1–8** were obtained from Metropolis Monte Carlo simulations (MMC) that were run with dielectric constants $\epsilon \approx 2\text{–}80$ using the GEGOP program. The results of the calculations agree well with the experimental data at dielectric constants of $\epsilon \approx 10$.

* Corresponding author.

INTRODUCTION

Sulfated oligo- and poly-saccharides are involved in a number of biological processes[1–12]. A major class of these sulfated polysaccharides are found in the glycosaminoglycans, like heparin, dermatan sulfate, and the chondroitin sulfates. Most glycosaminoglycans have a high density of negative charges expressed by their carboxylate and sulfate groups. A prominent example is heparin, which is involved in the blood clotting cascade and has a number of other physiological functions[2,3,5,6]. In heparin some of the sulfate groups of a specific pentasaccharide are essential for the binding to antithrombin III[13].

Charged interactions resulting from the presence of numerous charged functional groups could have a significant impact on the preferred conformations of biologically active oligosaccharides. The net effect of the charges on the preferred conformation of these carbohydrates could be either of a repulsive or attractive nature. Negatively charged groups that are close in space would normally exert repulsive interactions. However, if metal cations would be chelated between two negatively charged groups, attractive interactions could occur. Interactions between two charged groups in close proximity can possibly exert a very high energy contribution to the conformational state compared to other conformational influences. For example, two negatively charged groups that are 5 Å apart have a Coulomb interaction energy of 66 kcal/mol in vacuo and an interaction energy of 0.8 kcal/mol at a dielectric constant of 80, which is the macroscopic value for water. In contrast, normal torsional potentials have an amplitude of ≈ 3 kcal/mol. Thus, the interaction energies between charged groups could potentially be more important than all other interactions in a molecule in determining the low energy conformation.

Whether or not conformational changes would be induced in a carbohydrate by charged groups and the magnitude of these conformational changes depends on the effective charge visible by the other charged groups. The effective charge of a group visible to the outside is, among other factors, dependent on the time-averaged proximity of the cation. Whether the conformational changes result in a shorter or longer distance between the charged groups depends on whether a complexation with a cation occurs between the charges.

Different influences of charged groups on the conformation of saccharides have been reported. It has been shown, for example, that sulfate groups influence the ring conformation of 2-sulfated iduronic acid residues in heparin oligosaccharides[14–17]. Various amounts of $^2S_0$ conformations were found depending on the sulfation pattern of the neighboring *N*-acetylglucosamine residues. In contrast, monosulfation of the 6-position of glucose derivatives has no significant effect on the conformation of the C-5–C-6 linkage[18]. Also, the X-ray crystal structure of sucrose octasulfate[19] does not show any significant deviations from the X-ray crystal structure of sucrose itself[20]. However, it was shown recently that the glucuronate residue of chondrosine exists in a boat–chair equilibrium due to the

zwitterionic interactions in the molecule[21]. Recent developments for force-field parameters for sulfate groups of oligosaccharides have been reported to match the observed X-ray structures with high precision[22].

RESULTS AND DISCUSSION

The conformational changes of oligosaccharides caused by charge–charge interaction are described for two series of ionic disaccharides. One series consists of derivatives of the benzyl glycoside of β-D-Gal-(1 → 4)-β-D-GlcA (**1**), which are either sulfated at the 6′-position (**2**) or at the 4′-position (**3**) or disulfated at the 4′- and 6′-position (**4**) (Scheme 1). The other series consists of derivatives of the benzyl glycoside of β-D-GlcA-(1 → 3)-β-D-Gal (**5**), which are sulfated in the 6-position (**6**), 4-position (**7**) or disulfated in the 4- and 6-position (**8**) (Scheme 1). The synthesis of these compounds was reported elsewhere[23,24]. These disaccharides carry a carboxylate group on the glucuronate residue and zero, one, or two sulfate groups on the galactosyl residue and, as such, serve as models for the two repeating disaccharide blocks of the chondroitin sulfates. The β-(1 → 4)-linked compounds **2**, **3**, and **4** should have the sulfate group(s) and the carboxylate group on opposite sides of the molecule, if the molecules adopted a conformation similar

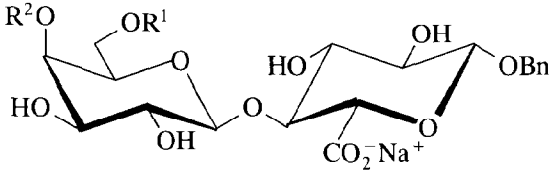

1 $R^1 = R^2 = H$
2 $R^1 = SO_3^-Na^+$, $R^2 = H$
3 $R^1 = H$, $R^2 = SO_3^-Na^+$
4 $R^1 = R^2 = SO_3^-Na^+$

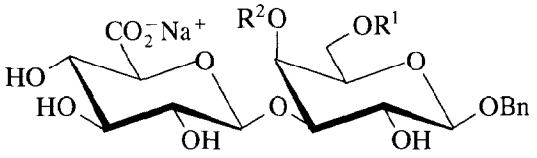

5 $R^1 = R^2 = H$
6 $R^1 = SO_3^-Na^+$, $R^2 = H$
7 $R^1 = H$, $R^2 = SO_3^-Na^+$
8 $R^1 = R^2 = SO_3^-Na^+$

Scheme 1.

to those described for uncharged β-(1 → 4)-linked disaccharides[25]. In the case of the β-(1 → 3)-linked disaccharides **6–8**, however, the sulfate groups and the carboxylate groups should be on the same side of the molecules, if the disaccharides adopt a conformation similar to those found in uncharged β-(1 → 3)-linked disaccharides[26]. The presence of a benzyl aglycon should not affect the preferred conformations of the glycosidic linkages in **1–8** and should exert only a small effect on the preferred conformation of the hydroxymethyl group in **5–8**. Also, the substitution of a galactosyl residue for an *N*-acetylgalactosaminyl residue should have little impact on the charge–charge interactions in the disaccharides studied.

Conformational analysis of sulfated derivatives of β-D-Gal-(1 → 4)-β-D-GlcA-O-Bn (**1–4**).—The conformations of the β-D-Gal-(1 → 4)-β-D-GlcA derivatives **1–4** have been analyzed by NMR spectroscopic techniques to determine the preferred conformational states of the molecules. The experimental results are compared to theoretical simulations of the sulfated structures **1–4**.

Conformation of the C-5–C-6 linkage of the galactosyl residue of **1–4**.—The $^3J_{H\text{-}5,H\text{-}6}$ coupling constants have been used to analyze the conformational preferences of the C-5′–C-6′ linkage. It has been shown that the unambiguous assignment of H-$6_{pro\text{-}R}$ and H-$6_{pro\text{-}S}$ is essential for a correct derivation of rotamer populations from the coupling constants[27]. The experimentally observed coupling constants for the galactosyl residue of **1–4** do not allow one to distinguish between the two different possibilities for the assignment. One assignment would result in a high population of the *gt* conformer, and the other would result in *tg* being the most dominant conformer (cf. Fig. 1). In galactopyranose the predominant conformer is the *gt* conformer[27,28]. However, we did not know of the effect of the charged groups on the preferred conformation of the hydroxymethyl groups in galactosyl residues. Thus, in the case of **4** the assignments of H-$6'_{pro\text{-}R}$ and H-$6'_{pro\text{-}S}$ have been made on the basis of NOE experiments with irradiation of H-4′. The NOEs from H-4′ to H-$6'_{pro\text{-}S}$ and to H-$6'_{pro\text{-}R}$ can be used in conjunction with the experimentally observed vicinal coupling constants $J_{H\text{-}5,H\text{-}6}$ to determine which proton is *pro-R* and which is *pro-S*. If the large NOE occurs for the proton that has a large vicinal coupling constant, it can be assumed that the hydroxymethyl group is preferentially in the *tg* conformation. If the proton with the small coupling constant shows the largest NOE, the hydroxymethyl group is preferably in the *gt* conformation. A prerequisite for the successful application of this technique is that

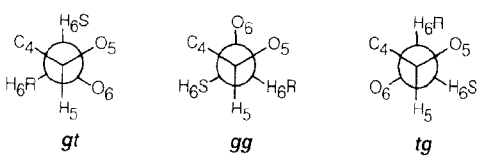

Fig. 1. Newman projections of the three staggered conformers found around the C-5–C-6 bond.

the coupling constants of H-5′ to H-6′$_{pro\text{-}R}$ and H-6′$_{pro\text{-}S}$ are very different. For **4** we observe in fact the larger NOE for H-6′, with the smaller coupling constant that assigns this proton as H-6′$_{pro\text{-}S}$ and the proton with the larger coupling constant as H-6′$_{pro\text{-}R}$. This determines at the same time that the preferred conformation is *gt* and agrees with the assignments made earlier for galactose derivatives[27,28]. The spin systems of H-5′, H-6′$_{pro\text{-}R}$, and H-6′$_{pro\text{-}S}$, and, in the case of **1** and **2** also H-4′, were analyzed by an iteration of the high-order spin system. The coupling constants and chemical shifts obtained from the high-order analysis are summarized in Table Ia and deviate by up to 1.9 Hz and 0.06 ppm from those published earlier based on first-order analysis[23,24].

The rotamer populations have been calculated using the Karplus-type equations of Gerlt and Youngblood[29] and of Streefkerk et al.[30] and are listed in Table Ia. The populations obtained from the two parametrizations of the Karplus equation differ maximally by up to $\approx 10\%$. However, the dependence of the rotamer population on the sulfation pattern is identical for both equations. The population of the hydroxymethyl group in the unsulfated **1** is very close to the values reported for free galactose[27,28,31]. The *gt* conformer is consistently found to be the predominant orientation of the 6′-group of **1**–**4**. The proportion of the *gt* conformation increases by about 8% in the case of the 4′-sulfate **3** and by about 18% in the case of the 4′,6′-disulfate **4**. The increase of the population of the *gt* conformer of **3** and **4** is accompanied by a decrease of the proportion of the *tg* conformer while the *gg* conformation's population remains nearly constant. For the 6′-sulfate **2** we observe a decrease of the population of the *gt* conformer by 10% and an increase of the population of the *tg* conformer by 6%.

The change of the population of the sulfonyloxymethyl group of **2** and **4** is interpreted straightforwardly in terms of charge–charge repulsions. Compound **2** shows an increase in the *tg* conformation, which places the two charged groups farthest apart. The population of the *gt* conformation which results in the sulfate group being closest to the carboxylate group is reduced. This change of the conformational preferences in the 6′-sulfate **2** is not caused directly by the substitution at C-6′ because 6-monosulfated derivatives of glucose show, for example, no effect in the change of the rotamer population relative to that of the unsulfated parent compound[18]. In the case of the 4′,6′-disulfate **4**, the charge–charge repulsion between the sulfate at the 4′-position and the sulfate at the 6′-position is responsible for an increase of the *gt* conformation relative to that of the unsulfated parent compound **1** and to **2**. This charge–charge interaction is stronger than the competing effect from the carboxylate, which is much further separated from the 6′-sulfate group than from the 4′-sulfate group. The increase of the *gt* rotamer of the hydroxymethyl group in the 4′-sulfate **3** by 8% is not as easily interpreted, but it is probably due to an increased dipolar effect between the C-4′–O4′ and the C-6′–O-6′ bond vectors.

The changes of the populations due to sulfation can be converted to energy differences between the individual staggered conformations (cf. Table Ia). The

highest populated conformation (*gt*) is set to a relative energy of 0.0 kcal/mol. The energy differences (ΔE) caused by the sulfation are consistent between the Gerlt and Youngblood and the Streefkerk parametrizations of the Karplus equation (Table Ia). The 6′-monosulfation in **2** destabilizes the *gt* conformer relative to **1** by ≈ 0.25 kcal/mol. The 4′-monosulfation in **3** destabilizes the *tg* conformer by ≈ 0.25 kcal/mol, while the *gg* conformer is unaffected. The 4′,6′-disulfation in **4** causes a significant destabilization of the *tg* conformer by ≈ 1.0 kcal/mol, whereas the data for the *gg* conformer are not conclusive, leading to a slight stabilization (−0.38 kcal/mol) with the Streefkerk parametrization and to a slight destabilization (0.10 kcal/mol) with the Gerlt–Youngblood parametrization.

Conformation of the glycosidic linkage in compounds **1–4** *as determined by NOE and ROE.*—NOEs and ROEs were recorded at 600 MHz because the spectral overlap in **1–8** did not allow an unambiguous interpretation of the NOEs at 300 MHz (see Fig. 2). At 600 MHz the NOEs are negative indicating that $\omega\tau_c > 1.12$. The magnitude of the NOEs at a sample temperature of 280 K and at a field strength of 600 MHz is relatively low. As a consequence, the correlation time of the molecules is close to the zero crossover point. Therefore, we also recorded one-dimensional ROEs that do not exhibit the problems originating from the zero crossover point of NOEs because ROEs are positive at all values of τ_c[32]. The experimental ROEs and NOEs are listed in Table IIa.

The NOE within the galactosyl ring from H-1′ to H-3′ was used as an internal reference. The NOE from H-1′ to H-5′ cannot easily be used because it is dependent on the relaxation of H-5′ with the H-6′-protons and is thus influenced by changes of the rotamer distribution of the C-5′–C-6′ bond. The largest NOE in all compounds is the interglycosidic NOE from H-1′ to H-4. The 4′-sulfate **3** exhibits an interglycosidic NOE from H-1′ to H-4, which is about 15% smaller than the same NOE of the unsulfated **1** (see Table IIa and Fig. 3). However, we observe that, relative to the unsulfated **1**, the NOE from H-1′ to H-4 is about 30% larger in the 6′-sulfate **2** and about 70% larger in the 4′,6′-disulfate **4**.

A similar trend is found for the intraglycosidic NOEs from H-1′ to H-5′, where the NOEs observed in **1** and in the 4′-sulfate **3** are of the same magnitude. The corresponding NOEs in the 6′-sulfate 2 and 4′,6′-disulfate 4 are both 60% larger than in **1**, reflecting the changes of the rotamer population of the C-5–C-6 bond (see above).

Additionally, in all compounds, two small interresidue NOEs upon irradiation of H-1′ can be observed to H-3 and H-5. Experimental interglycosidic NOEs from H-1′ to H-3 and H-5 show a dependence on the presence of sulfate groups. The ratios of the NOEs {H-1′}H-3 and {H-1′}H-5 are 0.6 for **1**, 1.1 for **2**, 0.7 for **3**, and 1.8 for **4**. These ratios indicate that the relative average distance from H-1′ to H-3 and H-5 are about the same in **1** and **3** whereas in **2** and **4** the distance from H-1′ to H-3 is significantly shorter and that from H-1′ to H-5 is longer than in **1**. This indicates that the 6′-sulfate group has a stronger influence on the conformation of the glycosidic linkage than the 4′-sulfate group.

TABLE Ia

^{1}H NMR chemical shifts and coupling constants of the H-5, H-$6_{pro\text{-}R}$ (labelled as H-6*R*), and H-$6_{pro\text{-}S}$ (labelled as H-6*S*) of **1–8** and experimental population of the C-5–C-6 linkage of the galactosyl residue derived therefrom [a]

	$J_{5,6R}$	$J_{5,6S}$	$\delta_{H\text{-}5}$	$\delta_{H\text{-}6R}$	$\delta_{H\text{-}6S}$	GY			S			GY		S		GY		S	
						gg	*gt*	*tg*	*gg*	*gt*	*tg*	E_{gg}	E_{tg}	E_{gg}	E_{tg}	ΔE_{gg}	ΔE_{tg}	ΔE_{gg}	ΔE_{tg}
1	8.12	4.68	3.576	3.596	3.645	19	56	25	8	66	26	0.61	0.45	1.18	0.52	0.00	0.00	0.00	0.00
2	7.30	5.20	3.857	4.109	4.094	24	45	31	12	56	32	0.35	0.21	0.86	0.31	−0.26	−0.24	−0.32	−0.21
3	8.62	3.99	3.718	3.664	3.676	19	64	17	11	71	18	0.68	0.74	1.04	0.77	0.07	0.29	−0.14	0.25
4	9.11	2.87	3.974	4.074	4.142	21	74	5	18	76	6	0.71	1.51	0.81	1.42	0.10	1.06	−0.38	0.90
5	7.82	4.41	3.530	3.611	3.647	23	54	23	15	62	23	0.48	0.48	0.79	0.56	0.00	0.00	0.00	0.00
6	8.47	3.41	3.771	4.059	4.083	23	65	12	19	69	12	0.58	0.95	0.72	0.98	0.10	0.47	−0.07	0.42
7	8.46	3.77	3.684	3.640	3.667	21	63	15	15	69	16	0.62	0.80	0.85	0.82	0.14	0.32	0.06	0.26
8	8.97	2.76	3.923	4.065	4.159	22	73	4	21	75	5	0.67	1.63	0.71	1.52	0.19	1.15	−0.08	0.96

[a] The Gerlt and Youngblood (GY)[29] and Streefkerk et al. (S)[30] parametrizations of the Karplus equation have been used to calculate the proportions of the *gg*, *gt*, and *tg* conformers. The experimentally derived populations have been used to calculate the differences in free energy (in kcal/mol) between the *gg* and the *gt* as well as between the *tg* and the *gt* conformations, respectively. The last four columns show the energy differences (in kcal/mol) between the sulfated structures **2–4** and **6–8** and the corresponding nonsulfated structures **1** and **5**. These columns are useful for assessing the effect of the sulfation on the relative stability of the conformers. The assignment for H-6*R* and H-6*S* were made on the basis of a combination of the coupling constants and the NOEs from H-4 to the H-6 protons. We observed for **4** NOEs from H-4′ to H-5′ = 0.61%, to H-6′*R* = 0.24% and to H-6′*S* = 0.38% and for **8** from H-4 to H-5 = 0.68%, to H-6*R* = 0.22% and to H-6*S* = 0.63%.

TABLE Ib

Calculated populations of the C-5–C-6 linkage of the galactosyl residue of **1–8** for various dielectric constants [a]

	1	**2**					**3**		**4**						**5**	
S	No	–	–	–	–	–	No	–	No	–	–	–	–	–	No	No
C		–	–	–	–	–		–		–	–	–	–	–		
ϵ		2	5	10	25	80		2		2	5	10	25	80		
gg	22	29	29	28	26	25	21	22	21	0	5	11	14	18	24	23
gt	64	32	47	50	59	61	64	65	64	93	86	79	76	66	65	59
tg	14	39	24	22	15	14	15	13	15	7	9	10	10	15	11	18

	6						**7**					**8**				
S	–	–	–	–	–	No	–	–	–	–	No	–	–	–	–	No
C	–	–	–	–	–		+	+	+	+		+	+	+	+	
ϵ	2	5	10	25	80		5	10	25	80		5	10	25	80	
gg	30	28	25	27	26	22	20	22	24	20	24	0	7	12	18	22
gt	68	68	64	62	60	61	62	64	63	61	61	50	71	72	65	66
tg	2	4	11	11	14	17	18	14	13	19	15	50	22	16	17	12

[a] The populations were obtained in Metropolis Monte Carlo simulations with 3×10^5 steps each and represent the cumulative populations of 0°–120° (*gt*), 120°–240° (*tg*), and 240°–360° (*gg*). The rows designated by S and C indicate the charges applied to the sulfate groups (S) and the carboxylate group (C). A minus sign (–) indicates a negative charge on the corresponding group; a "No" indicates a calculation without charges, and a plus sign (+) indicates use of a positive charge on the carboxylate group. The dielectric constant used in the MMC simulation is given in row ϵ.

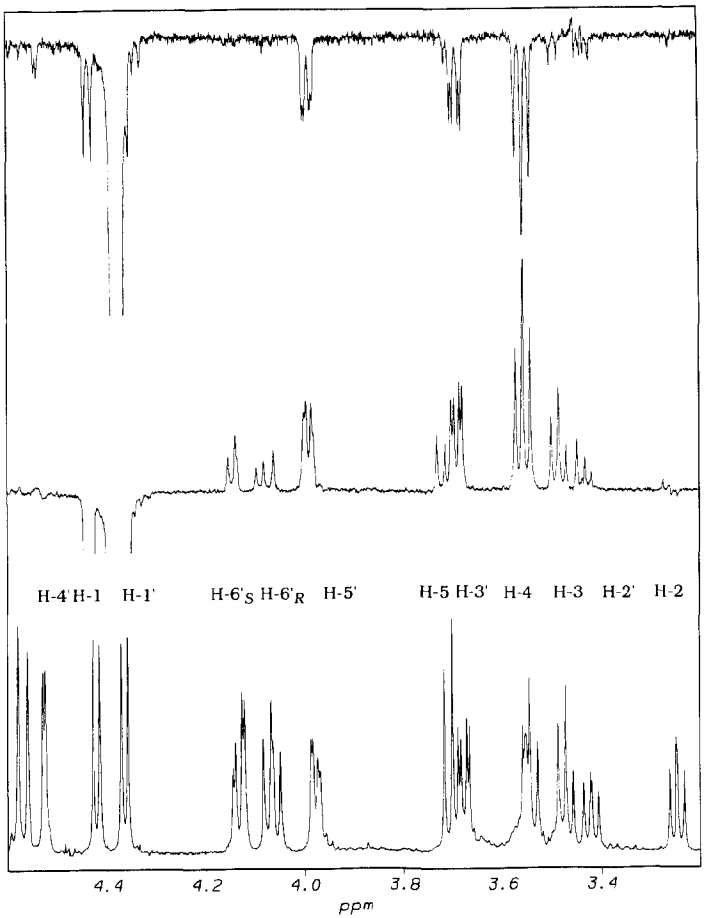

Fig. 2. Experimental ^{1}H NMR spectrum (lower trace), ROEs (middle trace), and NOEs (upper trace) of **4** at 600 MHz upon irradiation of H-1′ at 280 K. Only the region of the sugar proton resonances is shown.

The ROEs from H-1′ to H-4 support the findings from the NOEs in that **1** and **3** exhibit about the same ROE, whereas **2** and **4** show larger ROEs to H-4. The ROEs to H-3 and H-5 also show about the same ratio dependence on the sulfation pattern as discussed above for the NOEs (cf. Table IIa and Fig. 4) but are not easily quantified because of TOCSY transfers between the coupled signals.

Theoretical NOEs were calculated as a function of the correlation time using a full relaxation matrix approach[33] (cf. Table III and Fig. 5). The ratio of the theoretically derived intraresidue NOEs from H-1′ to H-3′ and to H-4′ varies from -0.23 at $\tau_c = 1 \times 10^{-10}$ s to 0.56 at 10×10^{-10} s. At a $\tau_c = 3 \times 10^{-10}$ s these NOEs are 0. These theoretically derived values are virtually independent of the conformation of the glycosidic linkage and can thus be compared to experimental values in order to derive an estimate of the correlation time τ_c of molecules **1–4**.

TABLE IIa

Experimental NOEs and ROEs for **1**–**8** at 600 MHz and 280 K [a]

	NOE								ROE							
	H-3′	H-4′	H-5′	H-6*R* + *S*	H-3	H-4	H-5		H-2′	H-3′	H-4′	H-5′	H-6*R* + *S*	H-3	H-4	H-5
1	1.00	0.12	0.58	0.00	0.06	0.95	0.10		0.20	1.00	0.05	1.27	0.00	0.20	1.33	0.60
2	1.00	0.11	0.95	0.22	0.07	1.20	0.06		0.25	1.00	0.16	1.21	0.25	0.59	1.42	0.23
3	1.00	0.14	0.57	0.00	0.09	0.80	0.12		0.23	1.00	0.08	1.16	0.38	0.23	1.26	0.36
4	1.00	0.19	0.93	0.05	0.15	1.63	0.08		0.27	1.00	0.03	0.94	0.63	0.50	1.70	0.27
	H-2′	H-3′ + H-4′	H-5′	H-2	H-3	H-4	H-6*R*	H-6*S*	H-2′	H-3′ + H-4′	H-5′	H-2	H-3	H-4		
5	0.11	1.09	1.00	0.25	1.10	0.09	n.d.	0.07	0.16	0.55	1.00	0.25	0.95	0.15		
6	0.19	1.23	1.00	0.26	1.26	0.21	0.15	0.26	0.24	0.65	1.00	0.28	1.06	0.16		
7	0.33	0.93	1.00	0.13	0.82	n.d.	0.00	n.d.	0.16	0.59	1.00	0.11	0.93	0.14		
8	0.29	1.01	1.00	0.08	0.98	n.d.	0.05	0.05	0.19	0.62	1.00	0.10	0.98	> 0.02		

[a] The values are given relative to H-3′ for **1**–**4** or to H-5′ for **5**–**8**, respectively. (For **5**–**8**, H-3′ is not a suitable reference because of signal overlap of H-3′ and H-4′.); n.d. values could not be integrated accurately.

TABLE IIb

Calculated NOEs for **1** to **8** [a]

	ϵ	H-2	H-3	H-4	H-5		ϵ	H-2	H-3	H-4	H-5
1	No	−0.76	−0.45	−7.25	−0.55	**5**	No	−1.03	−4.75	−0.97	−0.26
2	2	−0.92	−0.55	−8.51	−0.49	**6**	2	−1.40	−3.66	−0.61	−0.19
	5	−0.87	−0.50	−8.01	−0.52		5	−1.73	−4.26	−0.79	−0.23
	10	−0.84	−0.54	−7.65	−0.55		10	−1.18	−4.63	−0.86	−0.25
	25	−0.76	−0.51	−7.32	−0.56		25	−1.12	−4.88	−0.94	−0.26
	80	−0.77	−0.45	−7.31	−0.55		80	−1.03	−4.85	−0.96	−0.26
	No	−0.76	−0.44	−7.12	−0.55		No	−1.12	−4.78	−0.99	−0.26
3	2	−0.77	−0.45	−7.41	−0.51	**7**	2	−0.78	−5.48	−2.89	−0.40
	5	−0.77	−0.45	−7.42	−0.51		5	−0.84	−5.85	−1.55	−0.34
	10	−0.77	−0.44	−7.20	−0.53		10	−0.97	−5.42	−0.98	−0.29
	25	n.c.	n.c.	n.c.	n.c.		25	−0.98	−5.07	−0.79	−0.26
	80	n.c.	n.c.	n.c.	n.c.		80	−1.13	−4.84	−0.71	−0.25
	No	−0.79	−0.45	−7.33	−0.55		No	−1.16	−4.71	−0.67	−0.24
4	2	−0.95	−0.59	−8.73	−0.47	**8**	2	−0.70	−4.98	−1.24	−0.31
	5	−0.86	−0.51	−8.15	−0.50		5	−0.82	−5.38	−1.14	−0.31
	10	−0.80	−0.50	−7.73	−0.53		10	−0.92	−5.32	−0.93	−0.29
	25	−0.80	−0.46	−7.48	−0.54		25	−1.01	−5.04	−0.78	−0.27
	80	−0.76	−0.45	−7.19	−0.55		80	−1.03	−4.84	−0.70	−0.25
	No	−0.77	−0.45	−7.21	−0.56		No	−1.15	−4.35	−0.63	−0.22

[a] The values are obtained from Metropolis Monte Carlo simulations with 3×10^5 steps each. The $\langle r^{-3}\rangle$ matrix was sampled during the calculation and processed afterwards to give the calculated NOEs (cf. text). The simulations have been repeated with varying dielectric constants. Only interresidue NOEs are shown. The intraresidue NOEs are largely independent of the dielectric constant; n.c. = values not calculated because of small dependence of the conformational equilibrium on charge charge interactions.

The intraresidue NOEs calculated are H-2′ = −3.40, H-3′ = −6.15, H-4′ = −1.42, and H-5′ = −7.95 for **1**–**4** and H-2′ = −5.88, H-3′ = −4.28, H-4′ = −0.85, and H-5′ = −5.40 for **5**–**8**.

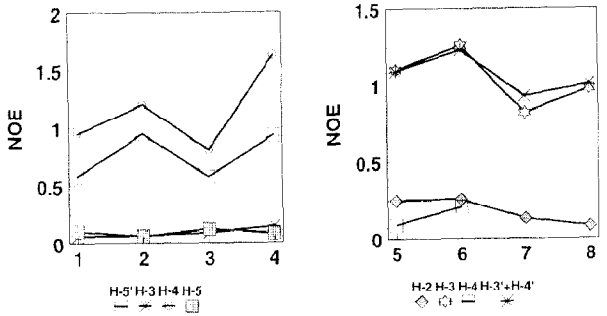

Fig. 3. Experimental NOEs of **1–8** at 600 MHz. Experimental NOEs to H-3, H-4, and H-5 across the glycosidic linkage and to H-5′ are expressed relative to the NOE to H-3′ for **1–4** (left panel) and NOEs to H-2, H-3, and H-4 across the glycosidic linkage and to H-3′ + H-4′ are expressed relative to the NOE to H-5′ for **5–8** (right panel).

The relative ratios of the intraresidue NOEs from H-1′ to H-3′ and from H-1′ to H-4′ were determined to be 0.12 for **1**, 0.11 for **2**, 0.14 for **3**, and 0.19 for **4**. These values correspond with correlation times of $3.5–4.0 \times 10^{-10}$ s, respectively. We find, not unexpectedly, the longest correlation time for the disulfated **4**. The estimates for the τ_c values correlate with the positive experimental NOEs observed at 300 MHz, and with the very small negative NOEs obtained at 500 MHz (not shown here). The NOEs are comparable across the series of compounds, because τ_c is about equal for **1–4**.

Conformation of the glycosidic linkage in compounds **1–4** *as determined from* ^{13}C *and* ^{1}H *NMR chemical shifts.*—The ^{13}C and ^{1}H NMR data of **1–4** have been reported elsewhere[23]. Changes of the ^{1}H NMR chemical shifts of **1–4** are indicative of the sulfation pattern (see Fig. 6). No further unusual chemical shift differences are observed. The direct effect of the sulfate groups on the ^{13}C NMR chemical shifts are as expected[34]. The C-4′ atoms show a downfield shift of 7.9 and

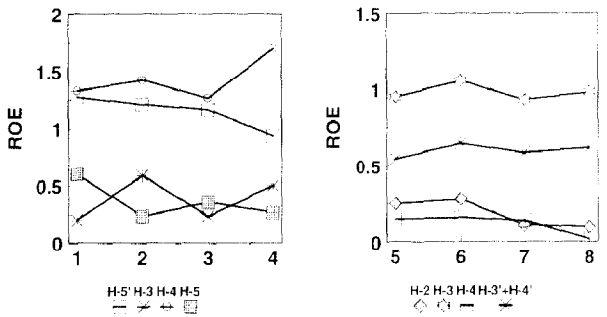

Fig. 4. Experimental ROEs of **1–8** at 600 MHz. Experimental ROEs to H-3, H-4, and H-5 across the glycosidic linkage and to H-5′ are expressed relative to the ROE to H-3′ for **1–4** (left panel) and ROEs to H-2, H-3, and H-4 across the glycosidic linkage and to H-3′ + H-4′ are expressed relative to the ROE to H-5′ for **5–8** (right panel).

TABLE III

Dependence of the calculated intraresidue NOEs upon irradiation of H-1′ on the correlation time of the molecule [a]

τ_c	**4**						**8**			
	H-2′	H-3′	H-4′	H-5′	H-6′R	H-6′S	H-2′	H-3′	H-4′	H-5′
1E−10	11.35	7.76	−1.87	11.68	−0.33	0.04	6.29	10.43	−1.81	16.31
2E−10	5.61	3.89	−0.27	5.51	−0.05	0.02	3.01	5.43	−0.04	7.85
3E−10	−0.20	−0.14	−0.01	−0.19	0.00	0.00	−0.11	−0.20	−0.02	−0.27
4E−10	−5.87	−4.28	−0.82	−5.41	−0.17	−0.13	−3.41	−6.15	−1.43	−7.97
5E−10	−11.40	−8.54	−2.46	−10.28	−0.58	−0.43	−7.09	−12.30	−4.00	−15.32
6E−10	−16.70	−12.84	−4.73	−14.84	−1.26	−0.98	−11.19	−18.48	−7.52	−22.27
7E−10	−21.69	−17.10	−7.42	−19.08	−2.21	−1.79	−15.62	−24.50	−11.70	−28.73
8E−10	−26.33	−21.22	−10.38	−23.02	−3.43	−2.88	−20.22	−30.24	−16.28	−34.68
9E−10	−30.61	−25.15	−13.46	−26.69	−4.91	−4.24	−24.87	−35.63	−21.05	−40.10
10E−10	*−34.54*	*−28.88*	*−16.58*	*−30.10*	−6.63	−5.85	−29.44	−40.62	−25.82	−45.00

[a] Data shown are for the disulfates **4** and **8** calculated without charges. Implementation of the full charges at $\epsilon = 2$ has no effect on the NOEs from H-1′ to H-2′, H-3′ and H-4′ and has only a slight influence on the NOEs from H′1 to H-5′, H-6′*S*, and H-6′*R*. The largest change from implementing full charges are ≈ 5% on H-6′*S* and 2% on H-6′*R*.

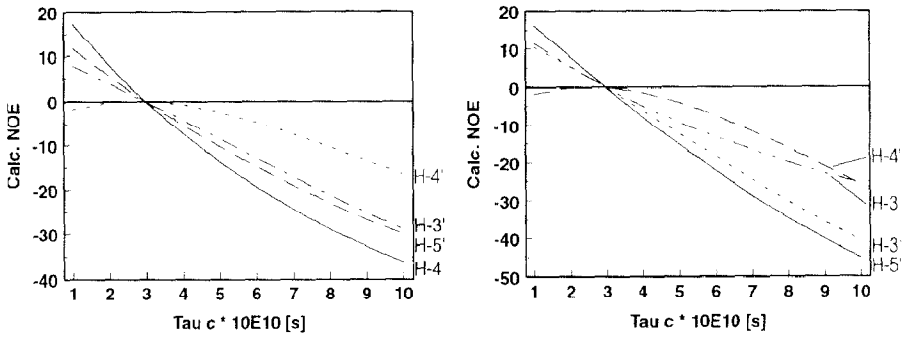

Fig. 5. Dependence of the calculated NOEs (600 MHz) on τ_c for **4** (left panel) and **8** (right panel). Intraring NOEs to H-3′, H-4′, and H-5′ and the major interresidue NOEs to H-4 (**4**) and H-3 (**8**), respectively, are shown.

7.6 ppm for **3** and **4**, respectively. The β-shift effect of the 4′-sulfate in **2** and **4** is between 0.7 and 1.3 ppm to higher field (see Fig. 7). The 6′-sulfate shifts C-6′ of **2** and **4** by 6.2 and 6.8 ppm to lower field. The β-shift effect of the 6′-sulfate group on C-5′ in **2** is 2.5 ppm to higher field. The 4′,6′-disulfate **4** shows a cumulative high-field shift effect on C-4′ of 2.9 ppm originating from both the 4′- and the 6′-sulfate groups.

However, other differences of ^{13}C NMR chemical shifts[23] between **1**–**4** have been observed that cannot be attributed to direct shift effects of the sulfate groups. However, they can be interpreted as being caused by conformational changes induced by the sulfation of the molecules. It is obvious from Fig. 7 that C-1′ and C-4 in **2** and **4** show a significant shift effect upon sulfation of the 6′-position. C-4 shows a shift to higher field of 1.4 ppm in **2** and a shift of 2.1 ppm in **4** and C-1′ a shift to lower field of 0.7 ppm in **2** and 0.8 ppm in **4** (see Fig. 7). Changes in chemical shifts of the carbon atoms adjacent to the glycosidic linkage have been demonstrated to correlate with changes in the conformation of the glycosidic linkage[35–37]. These correlations can be most accurately applied if a reference molecule with known chemical shifts is available. In our case we compare the sulfated structures **2**–**4** to the unsulfated derivative **1**. There should be no direct shift effect from the sulfate groups in the 4′-and 6′-positions on the chemical shifts of C-4 and C-1′, and in fact we do not find any change of these chemical shifts in the case of the 4′-sulfate **3**. Another indication of the high reproducibility of the ^{13}C NMR spectra are the differences in the chemical shifts observed for C-2, C-3, C-5, and C-2′. The changes found in **2** and **4** can be translated into changes of the preferred conformation of the glycosidic linkage using a slope of $\Delta\theta/\Delta\delta = 9°/\text{ppm}$ (refs. 35–37), resulting in changes of the ϕ angle of **2** by $-13°$ and that of **4** by $-19°$. The ψ angle changes for both molecules by $-6°$.

Metropolis Monte Carlo calculations of **1**–**4**.—We performed Metropolis Monte Carlo (MMC) calculations[38–42] on **1**–**4** with 3×10^5 steps each. Separate MMC simulations of **1**–**4** were run setting the dielectric constant to 2, 5, 10, 25, and 80,

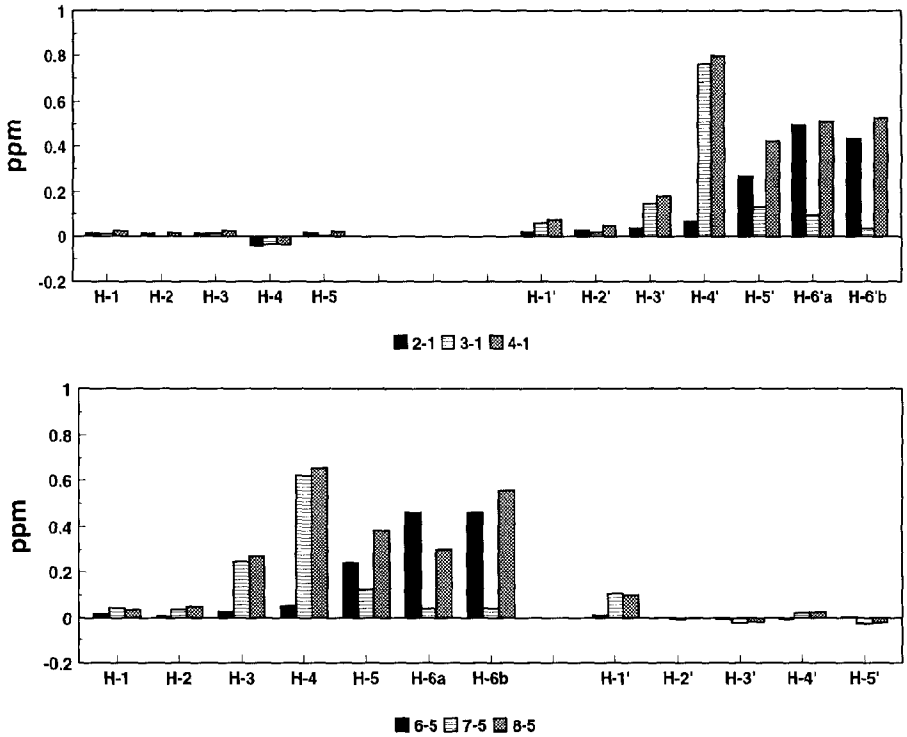

Fig. 6. Differences (in ppm) of the ^{1}H NMR chemical shifts of **2**–**4** (upper panel) and **6**–**8** (lower panel) relative to the unsulfated parent molecules **1** and **5**, respectively. The shift differences of H-1, H-2, H-3, and H-5 in the upper panel and of H-2′, H-3′, H-4′, and H-5′ in the lower panel can be used as indicators for the quality of the chemical shift calibration. Unusual changes of chemical shifts are observed for H-4 and H-1′ in the upper panel and for H-1′ in the lower panel. The changes of the chemical shifts of H-3′, H-4′, H-5′, and H-6′ in the upper panel and of H-3, H-4, H-5, and H-6 in the lower panel are direct effects from the substitution by sulfate groups.

respectively, thus effectively modulating the energy effect of the charged groups on the conformation of the disaccharides. The charges were distributed such that the carboxyl oxygens were carrying 0.5 negative charges each and the sulfate oxygens were carrying 0.33 negative charges each. For reference purposes we have also calculated **1**–**4** without any charges. MMC simulations allow an assessment of the dynamics of a molecule and the derivation of the average values of observable physical parameters that can be compared to experimental data. Traces of the dihedral angles ϕ, ψ, and ω of **1**–**4** as a function of the Monte Carlo step number (cf. Fig. 8) were used to assess whether the MMC simulations had reached thermodynamic equilibrium. A minimum of ≈ 10 transitions between individual conformational states are necessary to allow for a statistical analysis of the MMC traces[39]. In all calculations performed, the traces of the ω angles show numerous transitions between the three rotamers and thus indicate that thermodynamic equilibrium had been reached. The traces of the ϕ and ψ angles show that

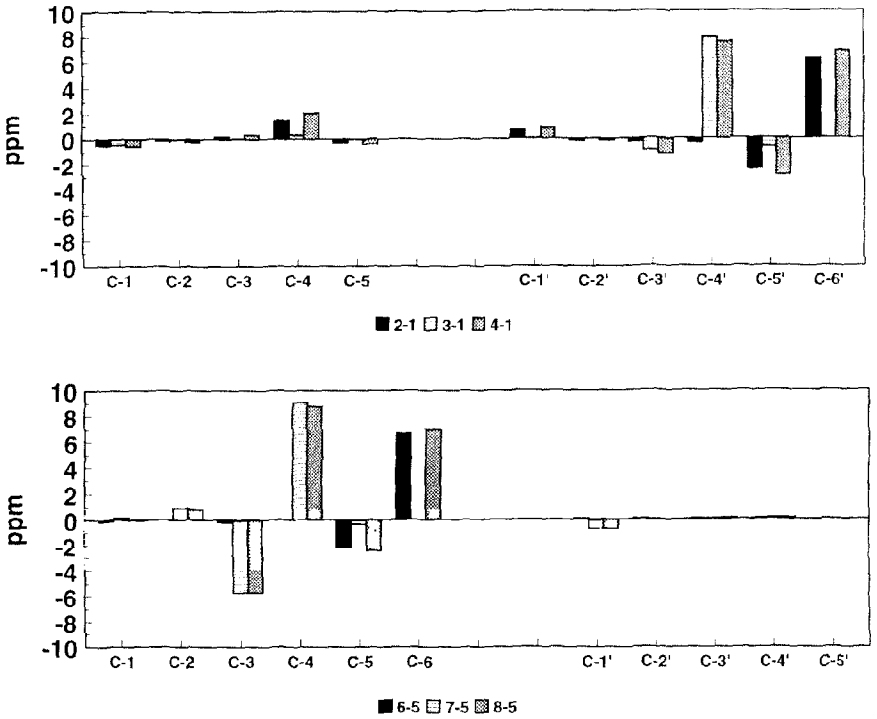

Fig. 7. Differences (in ppm) of the ^{13}C NMR chemical shifts of **2–4** (upper panel) and **6–8** (lower panel) relative to the unsulfated parent molecules **1** and **5**, respectively. The shift differences of C-2, C-3, and C-5 in the upper panel and of C-2′, C-3′, C-4′, and C-5′ in the lower panel can be used as indicators for the quality of the chemical shift calibration. Unusual changes of chemical shifts are observed for C-4 and C-1′ in the upper panel and for C-1′ and C-3 in the lower panel. The changes of the chemical shifts of C-3′, C-4′, C-5′, and C-6′ in the upper panel and of C-4, C-5, and C-6 in the lower panel are direct effects from the substitution by sulfate groups.

transitions between the main minimum at $\approx 60°/-10°$ and a side minimum at $\approx 165°/0°$ occur in many calculations but not in all. It is not clear whether the lack of the side minimum in some simulations is due to higher energies of that conformation and/or a different shape of the energy surface, or whether it is due to an incomplete scan of the conformational space.

For **1–4** we compared the rotamer populations of the C-5–C-6 bond obtained from the experimental coupling constants $J_{H\text{-}5,H\text{-}6}$ and the observed NOEs and ROEs across the glycosidic linkage with the corresponding theoretically derived average values. The populations of rotamers around the C-5–C-6 linkage are obtained from the trajectories of the MMC simulation (cf. Figs. 9, 10, and Table Ib). Furthermore, NOEs and ROEs are obtained from the average relaxation matrix, which in turn is obtained by updating the distance matrix (r^{-3}) (ref. 43) after each accepted step of the MMC simulation. Average NOEs and ROEs and

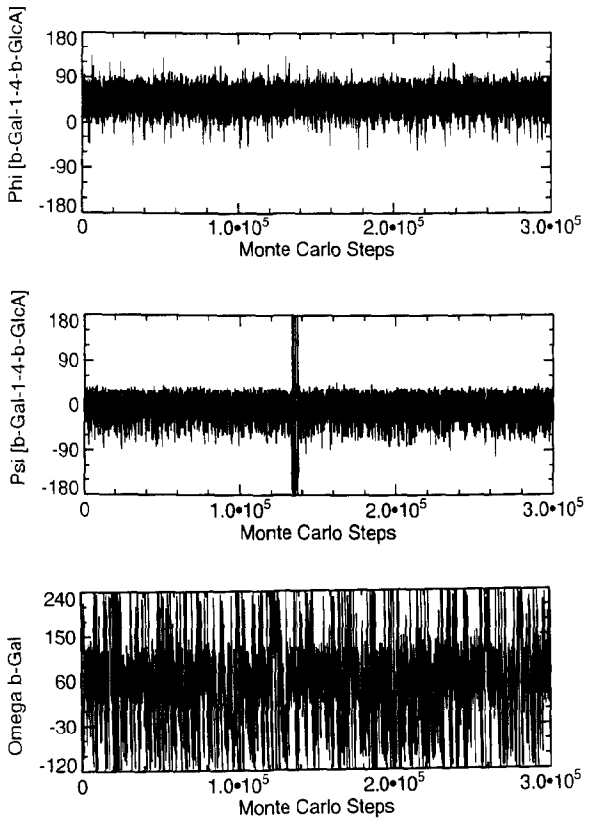

Fig. 8. Traces of ϕ, ψ, and ω of **2** as function of the Metropolis Monte Carlo step. Data were obtained from an MMC simulation with 3×10^5 steps with negative charges on the sulfate and carboxylate groups and $\epsilon = 10$. The number of transitions in the traces indicates the flexibility of the corresponding linkages. It is obvious that the C-5–C-6 linkage is the most flexible and shows multiple transitions during the simulation. The ψ angle shows only one transition.

populations around C-5–C-6 were obtained from different MMC simulations for **1–4** as a function of the dielectric constant ϵ. The expectation values obtained from the dynamics simulations of **1–4** that agree best with the experimental data were used to estimate the effective ϵ operative in aqueous solution. The conformational distributions at these points were used to describe the preferred three-dimensional structure(s) of **1–4** as a function of the sulfation/carboxylation and to describe the influence of these charged groups on the flexibility of the molecules.

The calculated rotational preferences of the C-5′–C-6′ linkage as a function of the effective charge on the sulfate and carboxylate groups are shown in Fig. 9. The interaction energy between the 6′-sulfate group and the carboxylate group in **2** and **4** can vary between 17.0 kcal/mol for $\epsilon = 2$ and 0.4 kcal/mol for $\epsilon = 80$ if the 6′-sulfate group is in the *tg* conformation and between 21.2 kcal/mol for $\epsilon = 2$ and 0.5 kcal/mol for $\epsilon = 80$ if the 6′-sulfate group is in the *gt* conformation. The interaction energy between the 4′-sulfate group and the 6′-sulfate group in **4** can

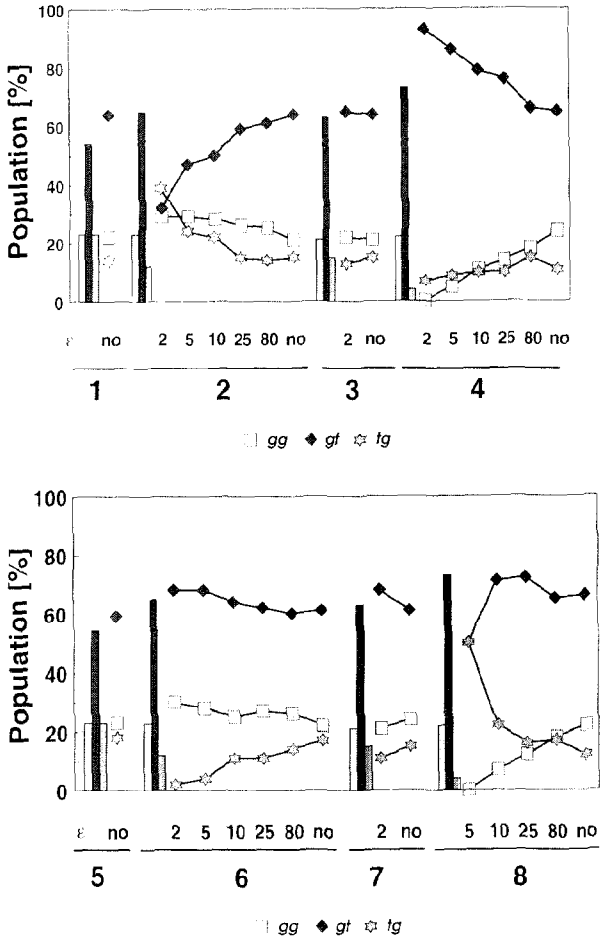

Fig. 9. Experimental and calculated populations of the C-5–C-6 linkages of the galactosyl residues for **1–4** (top panel) and **5–8** (bottom panel). Experimental values are represented as vertical bars. Theoretical populations were obtained as average values from Metropolis Monte Carlo simulations with different dielectric constants using 3×10^5 steps each. The values labeled "no" are derived from calculations that did not utilize charges; the other labels of the *x*-axis are the dielectric constants used in the MMC simulations. The calculations for **1–6** were carried out with all negative charges on the sulfate and the carboxylate groups. For **7** and **8** the calculated values were obtained with positive charges on the carboxylate and negative charges on the sulfate groups (cf. text). The best agreement between experimental data (bars) and theoretical data (lines and symbols) are found at dielectric constants around $\epsilon \approx 10$.

vary between 31.0 kcal/mol for $\epsilon = 2$ and 0.8 kcal/mol for $\epsilon = 80$ if the 6′-sulfate group is in the *tg* conformation and between 26.3 kcal/mol for $\epsilon = 2$ and 0.7 kcal/mol for $\epsilon = 80$ if the 6′-sulfate group is in the *gt* conformation. By comparing the calculated populations to the experimentally determined data, we find that the best fit of the theoretical with the experimental data is found at $\epsilon \approx 10$ (Table Ib and Figs. 9 and 10). At lower values of ϵ we calculate too large changes of the

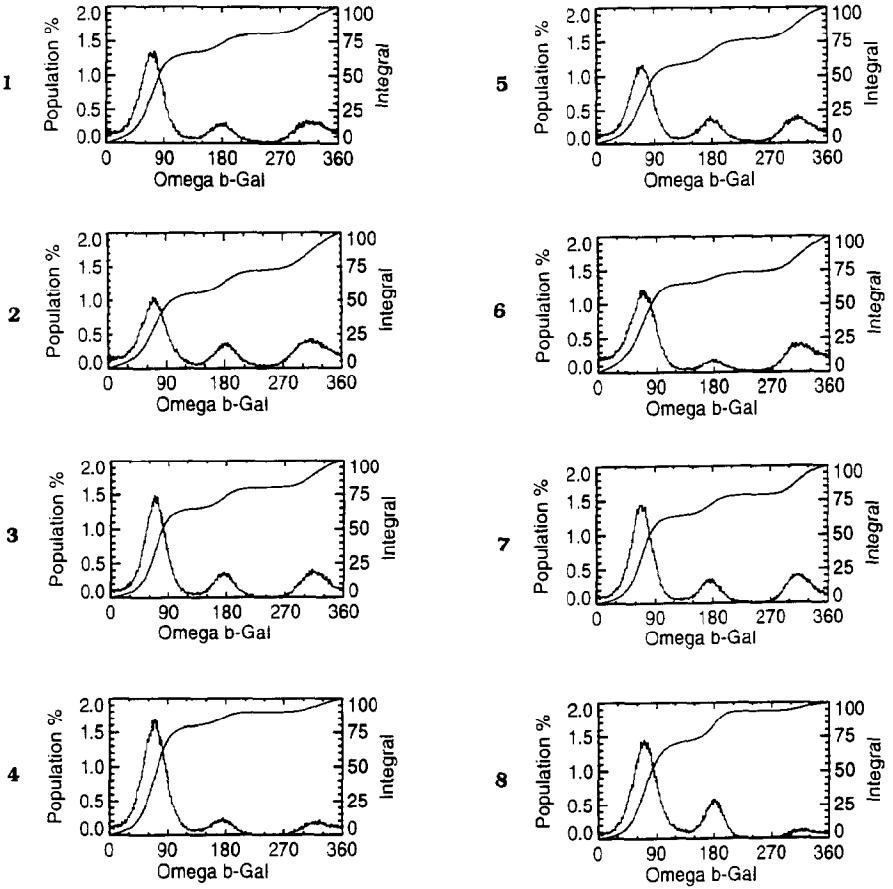

Fig. 10. Population plots of the C-5–C-6 linkage for **1–8** for a dielectric constant of $\epsilon = 10$ obtained from MMC simulations with 3×10^5 steps. The populations (left axis) were pooled in one-degree bins. The integral population (right axis) is also given.

conformational preferences of the C-5′–C-6′ linkage due to high interactions between the charges (e.g., **4** in Figs. 9 and 10). At higher values of ϵ the conformational preferences of **4** would not differ significantly from those of **1**. Neither of these agrees with the observed experimental data.

NOEs as a function of ϵ are listed in Table IIb and shown in Fig. 11. In comparison to **1**, it is obvious that the 4-sulfate **3** does not show a significant effect from the sulfate carboxylate interaction as the calculated NOEs from H-1′ to H-3, H-4, and H-5 do not change relative to those of the unsulfated **1**. This is because the distance between the sulfate group and the carboxylate group does not change significantly with a change of the conformation around the glycosidic linkage. As a result, no effect on the interglycosidic NOEs is observed.

The calculated NOE from H-1′ to H-4 of the 6-sulfate **2** shows a slight dependence on ϵ such that an increase in the NOE is calculated for smaller values

of ϵ. The ratio of the calculated NOE {H-1′}H-3 to {H-1′}H-5 does not change significantly as a function of the dielectric constant ϵ. Thus, the conformation of the glycosidic linkage is virtually independent of the charges on **2**.

In the 4′,6′-disulfate **4** three charge–charge interactions of two different types exist between the 6′-sulfate group and the 4′-sulfate group and between the carboxylate group and the 4′-sulfate and the 6′-sulfate groups. The distance between the 4′-sulfate and the 6′-sulfate group is shorter than that between the carboxylate and either sulfate group, resulting in a higher repulsive interaction between the sulfate groups. The 4′-sulfate group in **3** did not have a measurable conformational effect, and thus it is not expected that an effect from charge–charge interaction of the 4′-sulfate group with the carboxylate is important for the conformation of the glycosidic linkage of **4**. However, the interactions between the 6′-sulfate group and the carboxylate show their influence on the calculated conformational preferences as a function of the dielectric constant. We find in **4** that the calculated NOE from H-1′ to H-4 is calculated to be significantly larger than the analogous NOEs in **1** and **3** if the dielectric constant is set between $\epsilon = 2$ and $\epsilon = 10$. For **4**, at these values of ϵ, the calculated NOE of H-1′ to H-3 is equal to or larger than the NOE from H-1′ to H-5, which agrees with the experimental NOEs observed (compare Table IIb and Fig. 3). Of the compounds **2** and **4** that show a dependence on the dielectric constant in the calculation, we find the best agreement with the experiment at $\epsilon = 5$ to $\epsilon = 10$.

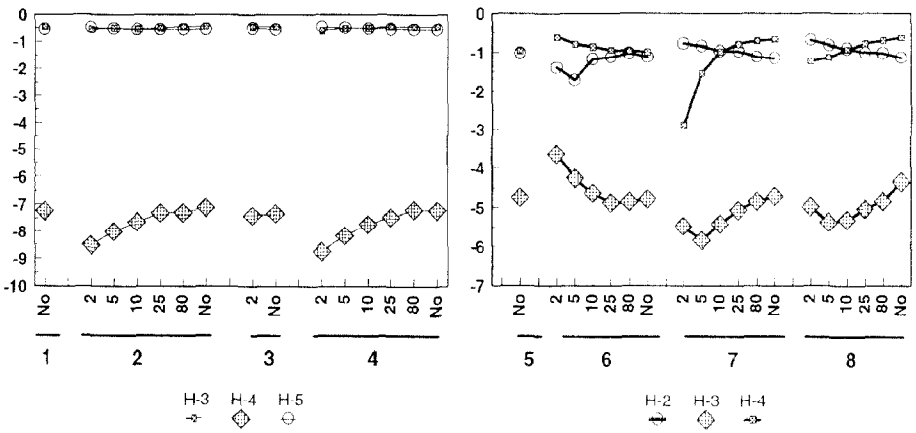

Fig. 11. Calculated NOEs across the glycosidic linkage for **1**–**4** (left panel) and **5**–**8** (right panel). The NOEs were obtained as ensemble average values from Metropolis Monte Carlo simulations with different dielectric constants using 3×10^5 MMC steps each. The distance matrices were sampled as $\langle r^{-3} \rangle$ values during the calculations and were processed using a full relaxation matrix approach. The values labeled "No" are derived from calculations that did not utilize charges. The calculations for **1**–**6** were carried out with all negative charges on the sulfate and the carboxylate groups. For **7** and **8** the calculated values were obtained with positive charges on the carboxylate and negative charges on the sulfate groups (cf. text).

TABLE IV

Average calculated dihedral angles ϕ and ψ for the glycosidic bonds and χ for the sulfate groups [a]

	S	C	ϕ	ψ	χ^6	χ^4
1		–	51 (23)	−3 (18)		
2	–	–	46 (18)	−9 (25)	177 (46)	
	No		52 (23)	−3 (18)	174 (56)	
3		–	52 (22)	−4 (17)		8 (15)
	No		50 (19)	−4 (18)		8 (15)
4	–	–	47 (17)	−9 (21)	171 (52)	11 (16)
	No		50 (20)	−3 (18)	172 (56)	9 (16)
5		–	50 (24)	−10 (25)		
6	–	–	50 (30)	−4 (25)	180 (56)	
	No		50 (25)	−11 (25)	179 (57)	
7	–	+	47 (17)	−17 (17)		8 (16)
	No		52 (16)	−2 (19)		11 (16)
8	–	+	50 (15)	−19 (15)	167 (71)	9 (16)
	No		59 (37)	−2 (18)	174 (59)	11 (16)

[a] The average values were obtained from 3×10^5 step MMC simulations. The standard deviations of the angles during the simulation is given in parenthesis. The calculations shown here were conducted with a dielectric constant of 10. The column labelled S shows the charges applied to the sulfate groups and that labelled C shows the charge applied to the carboxylate group; a minus sign (−) indicates a negative charge and a plus sign (+) a positive charge (cf. text). For reference purposes the calculations without charges (No) are also shown.

The preferred conformations of the disaccharides **1**–**4** at a dielectric constant of $\epsilon = 10$ are listed in Table IV. The flexibility of the molecules can be assessed from the standard deviations of the angles. As inferred from the standard deviations, which are a measure for the variability of the angles during the calculations, the inclusion of charges in the calculations does not significantly affect the flexibility of the angles. The changes of the dihedral angles ϕ and ψ calculated for **2** and **4** agree with the changes derived from the ^{13}C NMR and NOE data. The preferred structures of **4** calculated without charges and with negative charges on the sulfate and carboxylate groups are shown as stereopictures in Fig. 12. The effect of charges on the conformation of the glycosidic linkage is visible in **4** in that the two residues are rotated with respect to each other, resulting in the 6′-sulfate group and the carboxylate group being further apart than in the hypothetical uncharged **4**.

Conformational analysis of sulfated derivatives of β-D-GlcA-(1 → 3)-β-D-Gal-O-Bn (**5**–**8**).—The effect of the sulfation of the galactosyl residue on the conformation of the β-(1 → 3)-linked disaccharides has been studied for three different sulfated oligosaccharides **6**–**8** compared to the unsulfated parent compound **5**.

Conformation of the C-5–C-6 linkage of the galactosyl residue.—The $^3J_{H\text{-}5,H\text{-}6}$ coupling constants and NOEs from H-4 to H-6 were used to determine the

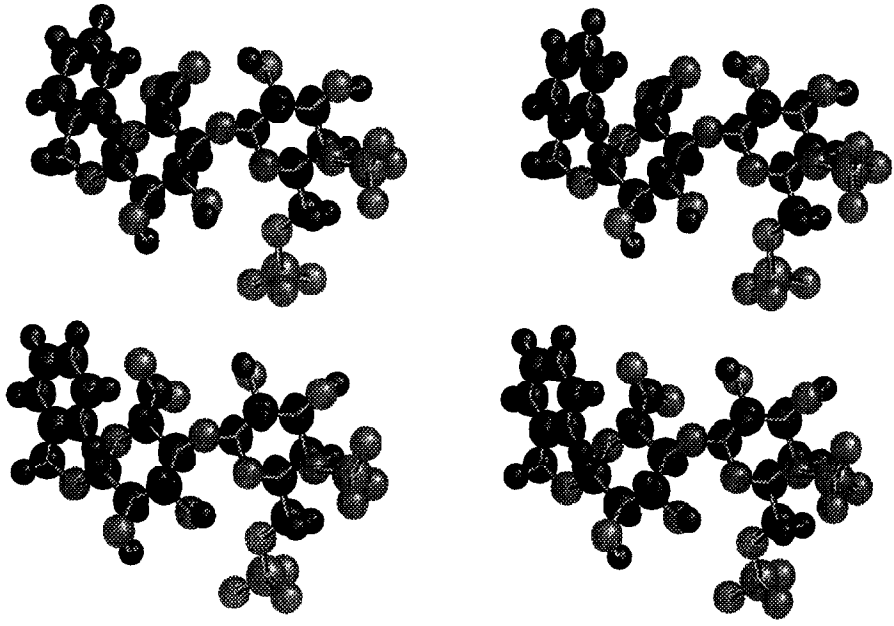

Fig. 12. Preferred average conformation of **4** as a stereo plot (ball-and-stick). Shown are the stereo pictures of the average structure calculated without charges (top) and that of the average structure calculated with negative charges on the sulfate groups and the carboxylate group with $\epsilon = 10$ (bottom). Black spheres indicate carbon and hydrogen atoms and gray spheres indicate oxygen and sulfur atoms.

conformational preferences of the hydroxymethyl or sulfonyloxymethyl group and their dependence on sulfation. The $^3J_{\text{H-5,H-6}}$ chemical shifts and coupling constants were obtained after an iterative analysis of the high-order spin systems made up by H-5, H-$6_{pro\text{-}R}$ and H-$6_{pro\text{-}S}$. H-$6_{pro\text{-}R}$ and H-$6_{pro\text{-}S}$ were assigned for **8** by measuring the NOEs from H-4 to H-6 (cf. above and Table Ia). The assignment of H-$6_{pro\text{-}R}$ and H-$6_{pro\text{-}S}$ in compounds **5–8** are in agreement with the assignments for compounds **2–4**, The NOEs clearly show that the C-5–C-6 linkage of the galactosyl residue of **8** has a preference for the *gt* conformer (cf. Table Ia).

We have used the same parameterizations of the Karplus equation[29,30] as for the β-(1 → 4)-linked disaccharides (cf. above) to calculate populations of the C-5–C-6 linkage from the experimental coupling constants (Table Ia). It is obvious from Table Ia that the two parameterizations of the Karplus equations give very similar results for the preferred populations of the C-5–C-6 linkage of **5–8**. The 4- or 6-sulfation of the galactosyl residue in **6** and **7** results in an increase of 10% of the *gt* conformer at the cost of the *tg* conformer. This is in contrast to the observations made for the β-(1 → 4)-linked 6′-sulfate **2** for which a decrease of the *gt* conformer's population was observed (cf. above). The combined effect of 4- and 6-sulfation in disulfate **8** gives approximately twice the effect as a monosulfation at these positions resulting in 73% *gt* and 4% *tg* conformers. The proportion of the *gg* conformer is not significantly affected by either 4- or 6-sulfation. The *tg*

conformation is not favored in the case of **6** and **8** because the 6-sulfate group would show electrostatic repulsion with the carboxylate group of the glucuronate residue.

The rotamer population of the C-5–C-6 linkage was converted into energy differences of the individual staggered conformers (cf. Table Ia) using Boltzmann statistics. The 6-sulfate group in **6** leads to a destabilization of the *tg* conformer by ≈ 0.4 kcal/mol, which is opposite to the effect observed for the 6′-sulfate **2**. The 4-sulfate group in **7** has an influence similar to that observed for the 4′-sulfate **3**, resulting in a slight destabilization of the *tg* conformer by ≈ 0.3 kcal/mol. The 4,6-disulfate **8** shows a strong destabilization of the *tg* conformer by ≈ 1 kcal/mol, which is similar to the destabilization observed for the 4′,6′-disulfate **4**.

Conformation of the glycosidic linkage of **5–8** *as determined by NOEs and ROEs.* —Overhauser enhancements, NOEs, and ROEs, obtained upon irradiation of H-1′ were used to determine the conformational preferences at the glycosidic linkage for **5–8**. The values reported in Table IIa are relative to the enhancement observed for H-5′, which was used as an internal reference. As a control we have also calculated the enhancements relative to the sum of H-3′, H-4′, and H-5′, which gave the same relative enhancements as that from using only H-5′ as a reference. Signal overlap of H-3′ with H-4′ prevents using H-3′ as an internal reference. Upon irradiation of H-1′, the strongest NOEs across the glycosidic linkage are observed to H-3. Small interresidue NOEs are observed for H-2 and H-4 of the galactosyl ring.

The presence of a 6-sulfate group in **6** leads to an increase of the {H-1′}H-3 NOE by 15% indicating a shorter distance between H-1′ and H-3. The presence of a 4-sulfate group in **7** leads to a decrease of the {H-1′}H-3 NOE by 25% compared to the unsulfated **5**, which indicates an increase in the average distance of H-1′ to H-3. Disulfate **8** exhibits a similar NOE to H-3 as the unsulfated parent molecule **5**. The small NOEs to H-2 and H-4 are very useful for an assessment of whether the glycosidic linkage has changed its preferences to one or the other side: i.e., whether H-1′ is closer to H-4 in time average than to H-2 or vice versa. The NOE from H- 1′ to H-2 for **5** and **6** is significantly larger than the NOE from H-1′ to H-4 (Table IIa and Fig. 3). Compared to **5** and **6**, the NOE from H-1′ to H-2 shows a marked decrease of 50 or 65% when a 4-sulfate group is present in **7** and **8**, respectively. This indicates that the conformation of the glycosidic linkage is not influenced by the presence of a 6-sulfate group but changes with the presence of a 4-sulfate group to result in a larger average distance between H-1′ and H-2. We have not been able to integrate the NOEs to H-4 in **7** and **8** because of their close proximity to the irradiation site.

The selective ROEs upon irradiation of H-1′ show the same dependence on the sulfation pattern as the NOEs (Table IIa and Fig. 4). The changes of the ROEs from H-1′ to H-3 as a function of the sulfation pattern in **5–8** are much smaller than the corresponding changes observed for the NOEs. Compound **6** shows $\approx 5\%$ higher ROE from H-1′ to H-3, whereas **7** shows $\approx 5\%$ less ROE to H-3 than **5** and

8, indicating that there are no major changes of the average distance between H-1′ and H-3 in dependence of the sulfation pattern. The relative ROEs to H-2 and H-4 upon irradiation of H-1′ show an identical behavior as the NOEs. The ratio of the ROE to H-2 vs. the ROE to H-4 is 1.6 for **5** and **6** but ≈ 0.8 for the 4-sulfate **7**. The ROE to H-4 in **8** cannot be quantitated because H-4 is too close to the irradiation site.

The ratio of the relative NOEs from H-1′ to H-3′ and to H-4′ is very dependent on the correlation time of the molecule (cf. Table III and Fig. 5) but independent of the conformation of the glycosidic linkage. Thus, it can be used to arrive at an estimate of the correlation time for **7** and **8**, for which the spectral dispersion was large enough to separately integrate the NOEs to H-3′ and H-4′. The experimental ratio of the NOE to H-3′ to the NOE to H-4′ is 4.2 for **7** and 4.1 for **8**. The ratio of the two NOEs is independent of the charge distribution of the aglycons of **7** and **8** and of the conformation of the glycosidic linkage. Thus, the experimental ratio can be compared to values calculated from the full relaxation matrix to arrive at $\tau_c \approx 4.0 \times 10^{-10}$ s for both **7** and **8**. This value agrees also with the fact that we observe slightly positive NOEs at 300 MHz (data not shown). The change of sign of the experimental NOE at 300 and 600 MHz can theoretically only be observed in the range of $\tau_c \approx 3.0 \times 10^{-10}$ s to $\tau_c \approx 6.0 \times 10^{-10}$ s. At 500 MHz we have observed extremely small negative NOEs (data not shown) for **5**–**8**, which requires a correlation time of greater than 3.5×10^{-10} s.

T_1 values were measured by nonselective inversion recovery for the unsulfated **5** and disulfate **8** at 500 MHz (see Table V). The T_1 values for both compounds **5** and **8** are comparable, especially for the protons with short relaxation times. Deviations for the protons with longer T_1 times are probably due to solvent relaxation with residual water.

Conformation of the glycosidic linkage of **5**–**8** *as derived from* ^{13}C *and* ^{1}H *NMR chemical shifts.*—The ^{13}C and ^{1}H NMR chemical shifts of **5**–**8** have been reported elsewhere[24]. The differences of the ^{13}C chemical shifts of the sulfated disaccharides **6**–**8** to the unsulfated parent molecule **5** are shown in Fig. 7. The small differences observed for C-2′ to C-6′ upon sulfation give an estimate of the error for the chemical shifts of the carbon atoms. It is obvious that the C-1′ atoms of the 4-sulfated **7** and the 4,6-disulfated **8** show a high-field shift of 0.7 ppm. Furthermore, the ^{13}C NMR chemical shifts of the corresponding signals of C-4 in **7** and **8** are shifted downfield by 9.05 and 8.78 ppm, respectively. This change in chemical shift is unusually large for the α-shift effect which is normally on the order of 8.2 ppm[34]. The high-field β-shift effect on carbon C-3 is also unusually large at 5.7 ppm. Normal values are reported to be in the range of 1.0–2.0 ppm[34]. However, the α- and β-shift effects of the 6-sulfate groups in **6** and **8** on C-6 and C-5 are in the normal range of 6.7 and -2.2 ppm, respectively. We also observed an unusual γ-effect on C-2 with a downfield shift of ≈ 0.9 ppm in **7** and **8**. The unusual differences in chemical shifts can all consistently be interpreted by a change of the conformation of the glycosidic linkage when a 4-sulfate group is present in **7** and **8**.

TABLE V

Observed and calculated T_1 values (s) of **5** and **8**. The T_1 values are almost independent on the degree of sulfation. Calculated T_1 values for **5** are given for comparison assuming a correlation time of $\tau_c = 4 \times 10^{-10}$ (cf. text). The experimental T_1 values were measured at 500 MHz and 298 K. The calculated T_1 values are determined from the conformational average of a MMC simulation of 3×10^5 steps

	5	**8**	Calcd for **5**
Gal			
H-1	0.88	0.84	1.13
H-2	2.10	2.25	5.23
H-3	0.76	0.64	0.95
H-4	0.94	0.87	1.36
H-5	0.64	0.64	0.93
H-6a	0.60	0.46	0.51
H-6b	0.59	0.54	0.58
Glc			
H-1	0.72	0.85	1.21
H-2	2.22	1.80	3.21
H-3	1.98	1.46	2.19
H-4	1.82	1.41	3.33
H-5	1.08	0.93	1.94
OBn			
Ha	0.87	0.84	0.56
Hb	0.90	0.90	0.58

Compared with galactose 4-sulfates, C-3 of **7** and **8** shows a β-shift effect to higher field that is about 3.7 ppm larger than expected for sulfate groups[44]. Interpreted in terms of a changed conformation at the glycosidic linkage[35–37], these unusual shift effects reflect a change of the glycosidic dihedral angle ϕ by $\approx 30°$ to smaller values. The change of the chemical shift of C-1′ can also be interpreted as a change in the conformation of the glycosidic ψ angle. The shift differences would require a small change of the ψ angle to smaller values by about 3–5°. The observed change in the chemical shift of C-2 in **7** and **8** is consistent with the change of the chemical shift at C-1′ if the rotation around ψ is to more negative angles. A rotation of about 5° should result in a change of the chemical shift of C-2 of about 1 ppm to lower field due to the γ-gauche effect, which is actually observed for **7** and **8**. The large chemical shift difference of C-4 in **7** and **8** is interpreted by a change of the conformation of the hydroxymethyl group to a higher proportion of *gt* conformers (cf. above), which should result in a low-field shift on C-4 due to the γ-gauche effect. The conformational changes expressed by the ^{13}C NMR shift differences of **7** and **8** would move the 4-sulfate and the carboxylate groups closer together.

Changes of the chemical shifts in the ^1H NMR spectra are largely due to the sulfation pattern of the galactosyl residue. However, in comparing to reference data for galactose and sulfated galactose derivatives[34] and to the values deter-

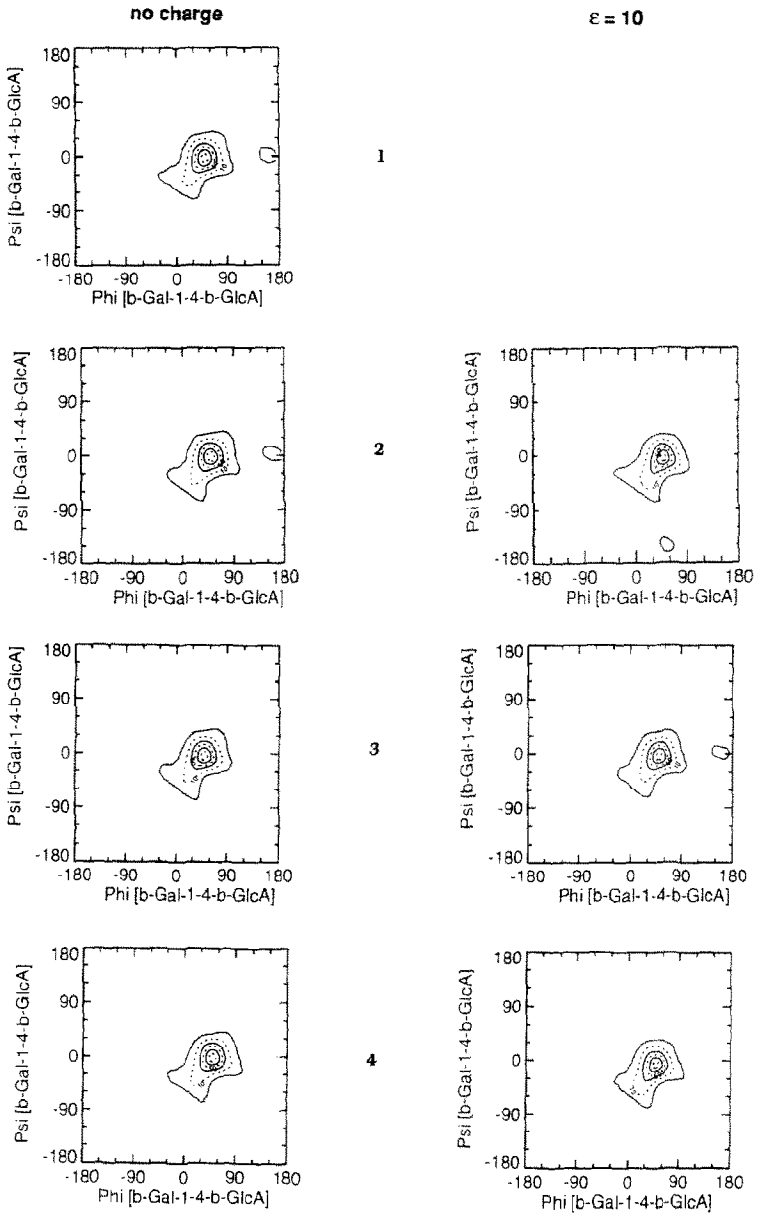

Fig. 13. Contour plots of the populations of ϕ and ψ as a function of the effective charge for (a) **1**–**4**, and (b) **5**–**8**. The data were obtained from MMC simulations with 3×10^5 steps each. Shown are the data for the simulations without charges (left) and for the simulations with charges and $\epsilon = 10$ (right). In **2**, **3**, **4**, and **6** all charges are negative and in **7** and **8** the charges on the carboxylate are positive (cf. text). After the MMC simulation the populations were sampled into bins of 6° length and are expressed in percent relative to the highest populated bin. The contour lines represent 1, 10, 30, 50, 70, and 90% relative population, respectively (outside to inside). The side minima at $\phi/\psi = 180°/0°$ and $60°/-150°$ do not occur in all contour plots. It is not clear whether this is an effect of not reaching full equilibrium in the MMC simulations or whether this is a real effect.

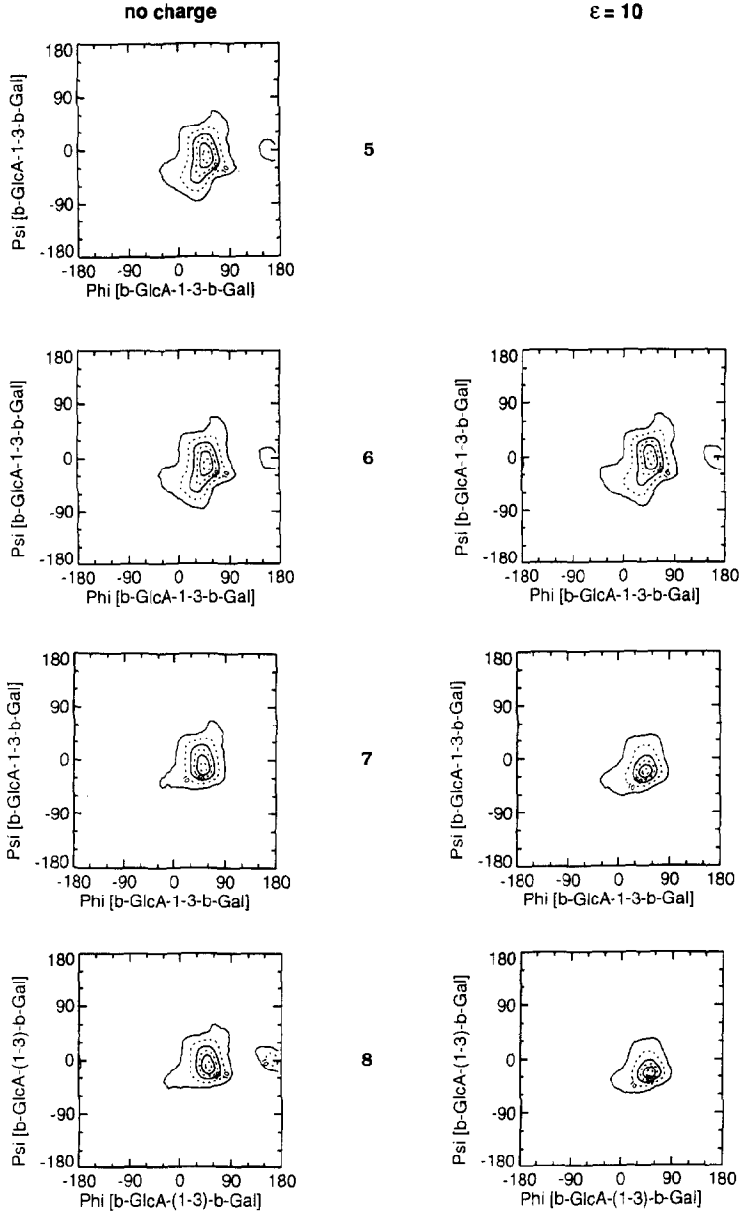

Fig. 13. continued.

mined for **2**–**4**, several differences become apparent. Due to the sulfation in **7** and **8**, H-4 shows an α-shift effect of ≈ 0.6 ppm, which is 0.2 ppm smaller than normally observed for a 4-sulfate group in a galactosyl residue (Fig. 6). The β-shift effects for H-5 are identical to those observed for **2**, **3**, and **4**. However, the other

β-proton, H-3, in **7** and **8** shows a shift effect that is ≈ 0.1 ppm further downfield than observed for 4-sulfated monosaccharides, and for **3** and **4**. The chemical shifts of H-1′ are most unusual in that they also show a downfield shift of 0.1 ppm in **7** and **8**. The chemical shift differences of H-2′, H-3′, H-4′, and H-5′ can be used to assess the reproducibility of the chemical shifts to ≈ 0.02 ppm. The unusual changes of the chemical shifts of H-1′ and H-3 are observed for **7** and **8** that also were showing unusual changes of the carbon chemical shifts. The 6-sulfate **6** does not show any unusual effects in the chemical shifts of H-1′ and H-3. The additional downfield shifts of H-1′ and H-3 in **7** and **8** are in agreement with a conformational change of the glycosidic linkage that brings the charged groups closer together.

Metropolis Monte Carlo calculations of **5–8**.—MMC calculations for **5–8** were performed as described above using dielectric constants of $\epsilon = 2$, 5, 10, 25, and 80. The values expected for the Overhauser effects and the populations around the C-5–C-6 linkages obtained from the MMC simulations with no charges or with all negative charges did not lead to agreements for all corresponding experimental data. Calculations with uncharged molecules resulted in the NOE from H-1′ to H-4 being calculated smaller than that to H-2, which is also found experimentally for **5** and **6**. However, the experimental data for the 4-sulfate **7** and the 4,6-disulfate **8** show the opposite effect in that the NOE {H-1′}H-4 is greater than {H-1′}H-2. Thus, it seems that the 4-sulfate group has a different influence on the conformation of the glycosidic linkage than the 6-sulfate group. If the MMC simulations were run with negative charges on all charged groups, the ratio of the NOE {H-1′}H-4 to the NOE {H-1′}H-2 was calculated at all dielectric constants to be even smaller than calculated for the uncharged case. This is in contrast to the experimental results for **7** and **8** where {H-1′}H-4 is greater than {H-1′}H-2. For example, a plot of the calculated NOEs as a function of the correlation time τ_c at $\epsilon = 2$ reveals that the NOE {H-1′}-4 is much less than the NOE {H-1′}H-2 at all τ_c (data not shown). Thus, the experimental data for **7** and **8** agree even less with the results of the calculations with negative charges expressed than with the simulations without charges. Also, the NOE to H-3 from H-1′ grows smaller with negative charges on all groups such that it is calculated to be less than that to H-2 in the case of $\epsilon = 2$. However, the experimental NOE to H-3 from H-1′ is the largest interresidue NOE. Thus, the experimentally determined preferred conformations for **7** and **8** can neither be explained by the absence of charge–charge interactions nor by repulsive charge interactions between the sulfate and the carboxylate groups as becomes evident from the MMC calculations.

However, it is conceivable that the carboxylate and one sulfate group show an attractive interaction via the mediation of a cation, i.e., sodium. Therefore, we have also conducted MMC simulations with negative charges on the sulfate groups and positive charges on the carboxylate groups to simulate the effect of chelation of the sodium ion with the carboxylate and a sulfate group.

The calculated conformational preferences of the C-5–C-6 linkage as a function of the dielectric constant in **5–8** are shown in Fig. 9 and Table Ib. The interaction

energy between the 6-sulfate group and the carboxylate group in **6** and **8** can vary between 23.6 kcal/mol for $\epsilon = 2$ and 0.6 kcal/mol for $\epsilon = 80$ if the 6-sulfate group is in a *tg* conformation, and between 19.4 kcal/mol for $\epsilon = 2$ and 0.5 kcal/mol for $\epsilon = 80$ if the 6-sulfate group is in the *gt* conformation. For **6**, the best fit between the experimentally determined and the calculated populations is found in MMC simulations with negative charges on the sulfate and carboxylate group at $\epsilon \approx 10$ (Table Ib and Fig. 9). For **8** we find the best agreement for calculations that have attractive charge interactions between the 4-sulfate group and the 6'-carboxylate group and repulsive interactions between the two sulfate groups. As expected, the conformation of the C-5–C-6 linkage of the 4-sulfate **7** does not show any significant conformational changes dependent on the dielectric constant.

For the reasons described above, theoretical NOEs of **7** and **8** were calculated with negative charges on the sulfate groups and positive charges on the carboxylate group at $\tau_c \approx 4.0 \times 10^{-10}$ s as a function of the dielectric constant (cf. Table IIb). The best fit between the experimental data and the MMC simulations is found at $\epsilon \approx 10$. In **8** the NOE from H-1′ to H-3 is calculated to be the largest interglycosidic NOE with a magnitude of $\approx 60\%$ of the NOE from H-1′ to H-5′. The ratio of the relative NOEs to H-2 and H-4 is calculated to 0.7 at $\epsilon = 10$. The same trends are calculated for **7**. The NOEs and ROEs to H-2 for **7** and **8** are calculated to be smaller than those for **5** and **6**, which is also in good agreement with the experimental data. Thus, the attractive interactions between the 4-sulfate group and the carboxylate group in **7** and **8** bring the two charged groups closer together and effect a conformational change at the glycosidic linkage, which is in agreement with the observed changes in chemical shifts and NOEs (cf. Fig. 14). This change can also explain the reduction of the *tg* conformer in **7** compared to **5**, because the space available for the *tg* conformer of the hydroxymethyl group is significantly reduced by this conformational change (cf. Fig 9). The 6-hydroxymethyl group would come into close contact with the carboxylate group in a *tg* conformation.

Comparison of the results of the calculations of the unsulfated parent molecule **5** with the 6-sulfate **6** computed without any charges on the ionic groups shows that the 6-sulfate group does not restrict the conformational flexibility of the glycosidic linkage (Fig. 13). However, presence of a 4-sulfate in **7** and **8** restricts the glycosidic linkage somewhat in its flexibility. This effect is significantly amplified if charges are used in the calculations. The ϕ, ψ contour plots of **7** and **8** that contain a 4-sulfate group indicate that the area around $30°/-60°$ is no longer accessible.

The average values for the dihedral angles as obtained from MMC simulations are listed in Table IV. The changes of the dihedral angles of the glycosidic linkage (ϕ and ψ) calculated for the 4-sulfate **7** and the 4,6-disulfate **8** compared to those of the unsulfated **5** are in qualitative agreement with the experimentally observed changes obtained from the interpretation of the ^{13}C NMR chemical shifts and NOEs supporting the fact that the 4-sulfate group and the 6′-carboxylate group have a small attractive interaction. It becomes obvious that the interactions between the charged groups result in less flexible conformations for **8** as deduced

from the standard deviations of the dihedral angles. The C-1′–O-1 linkage seems to be more affected than the O-1–C-3 linkage.

The calculated conformations for **5**, **7**, and **8** obtained as averages from the MMC simulations are depicted in Fig. 14. For **7** and **8** the average structures of the simulations for the uncharged molecules are compared to those obtained with negative charges on the sulfate groups and with a positive charge on the carboxylate group for $\epsilon = 10$. The simulations for the uncharged molecules **7** and **8** compared to **5** show the effects of nonbonded interactions, whereas comparison of the simulations without charges and to those made with charges indicates the effect of the charge–charge interactions. it is evident that the two pyranose rings in **7** and **8** are rotated relative to each other such that the 4-sulfate group comes in closer contact with the 6′-carboxylate group.

CONCLUSION

The conformational effects of the interactions between sulfate and carboxylate groups in **1**–**8** are relatively small. The energy differences between different possible conformational states are on the order of 1 kcal/mol. This leads to the conclusion that charged groups even in highly charged molecules do not necessarily have to dominate the three-dimensional structure of the oligosaccharide. If a carboxylate and a sulfate group are in a conformational arrangement that favors the formation of a cationic bridge, we believe that such a bridge may easily be formed and that the cation compensates the negative charges to a large extent. This effect probably requires one of the interacting charged groups to be a carboxylate group as carboxylates are better ligands to cations than sulfates. Compensation of the charges could in turn lead to virtually no interaction between the complexed groups on one hand and other negatively charged groups on the other hand. This conclusion has also some bearing on the extrapolation of charge effects to the conformation of polymers like chondroitin-4,6-disulfate. In the polymeric chondroitin-4,6-disulfate both types of interactions, that is attractive and repulsive, can theoretically occur. Sulfate groups can interact with carboxylate groups that are fairly distant to result in slight repulsive interactions or sulfate groups can interact with carboxylate groups in close proximity such that, via a salt bridge, attractive interactions result in a compensation of the charges of the interacting groups (cf. Fig. 15). Extrapolated from the disaccharides, the attractive interaction in the polymeric chondroitin sulfates will probably be stronger than the

Fig. 14. Stereo representation of the ball-and-stick models of (A) **5**, (B), and (C) **7**, and (D) and (E) **8** obtained as average structures from MMC simulations. For **7** and **8** the structures of the simulations without [B and D] and with charges and a dielectric constant of $\epsilon = 10$ [C and E] are shown. Black spheres indicate carbon and hydrogen atoms, and gray spheres indicate oxygen and sulfur atoms. The molecules are oriented such that the galactosyl residue is always in the same orientation to the viewer. Comparison of B with C and of D with E show a small effect arising from charge charge interactions in that the molecules rotate in a way that brings the 4-sulfate and the carboxylate group closer together.

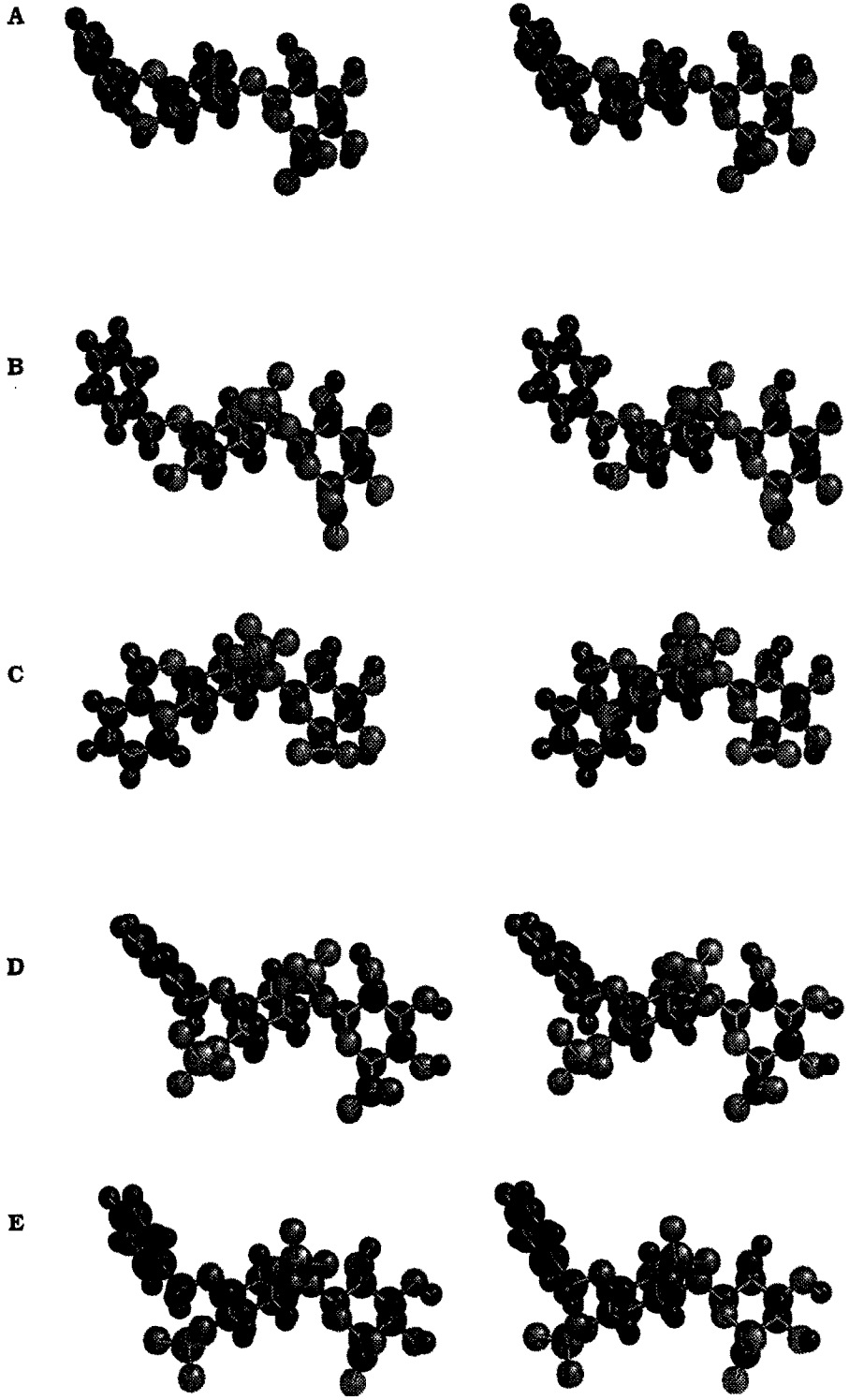
A
B
C
D
E

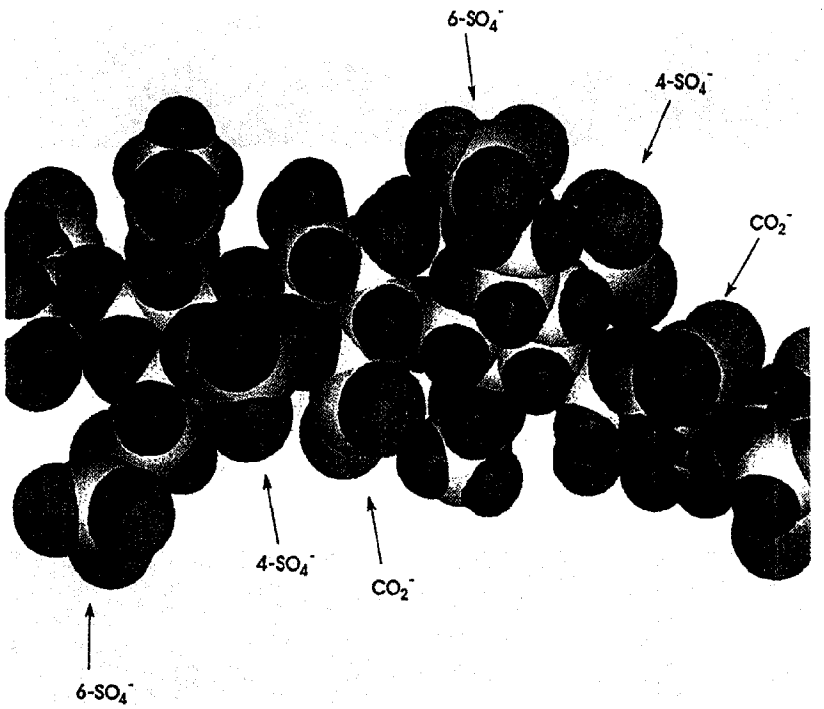

Fig. 15. CPK model of a section of a chondroitin-4,6-disulfate polymer calculated with the average angles obtained from the MMC simulations with $\epsilon = 10$ for **4** and **8**, respectively.

repulsive interaction leading to a compensation of the charges of the 4-sulfate groups and the carboxylate groups leaving the 6-sulfate groups largely unaffected. The attractive interactions would lead to an increase in rigidity of the β-(1 → 3) linkage, whereas the flexibility of the β-(1 → 4) linkages would be largely unaltered compared to the uncharged case. Also, the 6-sulfates in the polymeric chondroitin-4,6-disulfate should not show any significant interactions as they are three glycosyl residues apart and on opposite sides of the molecule (cf. Fig. 15).

EXPERIMENTAL

Dihedral angles are defined as follows: ϕ = H-1′–C-1′–O-1′–C-x, ψ = C-1′–O-1′–C-x–H-x, ω = O-6–C-6–C-5–O-5, χ^6 = S–O-6–C-6–C-5 for 6-sulfates, and χ^4 = S–O-4–C-4–H-4 for 4-sulfates. Positive angles are equivalent to a clockwise rotation.

The NOEs and the ROEs were measured on a 600 MHz NMR spectrometer (Bruker AMX 600), and the NOEs measured for the assignment of H-$6_{pro\text{-}R}$ and H-6_{pro-S} on a 250 MHz NMR spectrometer (Bruker AM 250). The solutions of **1–8** were salt free in D_2O containing 5% acetone-d_6 and had a concentration of 8–21 mmol/l. The samples were degassed by passing nitrogen through the solution. Removal of residual HDO was achieved by repeatedly dissolving the sample

in D_2O and freeze-drying. Selective ROEs where measured using a DANTE pulse train and a weak unshifted spin lock field of about 2500 kHz with a mixing time of 200 ms. NOE difference spectra where obtained by direct subtraction of the reference FID by phase cycling. The NOEs were observed as steady-state experiments with an irradiation time of 800 ms. T_1 values were obtained by the inversion recovery method at 500 MHz (Bruker AM 500) with delays from 10 μs to 10 s, and the T_1 values were calculated with the Bruker software using the exponential fit option. Spectra simulations of the H-5, H-$6_{pro\text{-}S}$, and H-$6_{pro\text{-}R}$ spin systems were performed using the program PANIC on a Bruker Aspect 3000 computer.

The theoretical calculations were done using the program GEGOP[38], Metropolis Monte Carlo simulations were run over 3×10^5 total steps with an acceptance rate of $\approx 40\%$ with a temperature parameter of 600 K. MMC calculations were run with effective charges of 0.0 or -0.33 on the oxygen atoms of the sulfate groups and 0.0, $+0.50$ or -0.50 on the oxygen atoms of the carboxylate group. Dielectric constants $\epsilon = 2$, 5, 10, 25, and 80 were used in the MMC calculations. The NOEs and ROEs were calculated from averaged relaxation matrices that were sampled over the 3×10^5 step MMC simulations. The relaxation matrices were subsequently processed to calculate the theoretical steady state NOEs by using a Gauss elimination[45] or the ROEs by using the eigenvalue procedure[45].

ACKNOWLEDGMENTS

We thank Dr. J. Glushka, Complex Carbohydrate Research Center, University of Georgia, for his assistance in setting up the ROE experiments and many valuable discussions.

REFERENCES

1 D. Comper and T.C. Laurent, *Physiol. Rev.*, 58 (1978) 255–315.
2 U. Lindahl and M. Höök, *Annu. Rev. Biochem.*, 47 (1978) 385–417.
3 B. Casu, *Adv. Carbohydr. Chem. Biochem.*, 43 (1985) 51–134.
4 G.A. Maresh, *Arch. Biochem. Biophys.*, 233 (1984) 428–437.
5 L. Thunberg, G. Bäckström, and U. Lindahl, *Carbohydr. Res.*, 100 (1982) 3939–410.
6 B. Casu, P. Oreste, G. Torri, G. Zoppetti, J. Choay, J.-C. Lormeau, M. Petitou, and P. Sinaÿ, *Biochem. J.*, 197 (1981) 599–609.
7 G. Bengtsson, T. Olivecrona, M. Höök, J. Riesenfeld, and U. Lindahl, *Biochem. J.*, 189 (1980) 625–633.
8 P. Avogaro and F. Belussi, *Pharmacol. Res. Commun.*, 9 (1977) 391–396.
9 D.D. Roberts, *Methods Enzymol.*, 138 (1987) 473–483.
10 E.D. Green, H. van Halbeek, I. Boine, and J.U. Baenziger, *J. Biol. Chem.*, 260 (1985) 15623–15630.
11 G.S. Bedi, W.C. French, and O.P. Bahl, *J. Biol. Chem.*, 257 (1982) 4345–4355.
12 E.F. Neufeld and G. Ashwell, in W.J. Lennarz (Ed.), *The Biochemistry of Glycoproteins and Proteoglycans*, Plenum Press, New York, 1980, pp 241–266.
13 M. Petitou, J.-C. Lormeau, and J. Choay, *Eur. J. Biochem.*, 176 (1988) 637–640.
14 G. Torri, B. Casu, G. Gatti, J. Choay, J.-C. Jacquinet, and P. Sinaÿ, *Biochem. Biophys. Res. Commun.*, 128 (1985) 134–140.

15 D.R. Ferro, A. Provasoli, M. Ragazzi, B. Casu, G. Torri, V. Bossenec, B. Perly, P. Sinaÿ, M. Petitou, and J. Choay, *Carbohydr. Res.*, 195 (1990) 157–167.
16 C.A.A. van Boeckel, S.F. van Aelst, G.N. Wagenaars, J.-R. Mellema, H. Paulsen, T. Peters, A. Pollex, and V. Sinnwell, *Recl. Trav. Chim. Pays-Bas*, 106 (1987) 19–29.
17 H. Paulsen, A. Pollex, V. Sinnwell, and C.A.A. van Boeckel, *Liebigs Ann. Chem.*, (1988) 411–418.
18 B. Meyer and R. Stuike-Prill, *J. Org. Chem.*, 55 (1990) 902–906.
19 Y. Nawata, K. Ochi, M. Shiba, K. Morita, and Y. Iitaka, *Acta Crystallogr., Sect. B*, 37 (1981) 246–249.
20 G.M. Brown and H.A. Levy, *Acta Crystallogr. Sect. B*, 29 (1973) 790–797.
21 D. Lamba, A. Segre, M. Ragazzi, D. Ferro, and R. Toffanin, *Carbohydr. Res.*, 209 (1991) C13–C15.
22 J.Y. Le Questel, C. Meyer, A. Imberty, and S. Perez, *Symposium on Conformational Studies of Oligosaccharides, Polysaccharides and Glycoconjugates*, Le Croisic, 1992, Abstr. III-10.
23 M. Zsiška and B. Meyer, *Carbohydr. Res.*, 215 (1991) 261–277.
24 M. Zsiška and B. Meyer, *Carbohydr. Res.*, 215 (1991) 279–292.
25 M.L. Hayes, A.S. Serianni, and R. Barker, *Carbohydr. Res.*, 100 (1982) 87–101.
26 N.B.N. Rao, V.K. Dua, and C.A. Bush, *Biopolymers*, 24 (1985) 2207–2229.
27 Y. Nishida, H. Ohrui, and H. Meguro, *Tetrahedron Lett.*, 25 (1984) 1575–1578.
28 H. Ohrui, Y. Nishida, H. Higuchi, H. Hori, and H. Meguro, *Can. J. Chem.*, 65 (1987) 1145–1153.
29 J.A. Gerlt and A.V. Youngblood, *J. Am. Chem. Soc.*, 102 (1980) 7433–7438.
30 D.G. Streefkerk, M.J.A. de Bie, and J.F.G. Vliegenthart, *Tetrahedron*, 29 (1973) 833–844.
31 H. Ohrui, Y. Nishida, M. Watanabe, H. Hori, and H. Meguro, *Tetrahedron Lett.*, 26 (1985) 3251–3254.
32 D. Neuhaus and M. Williamson, *The Nuclear Overhauser Effect in Structural and Conformational Analysis*, VCH, Weinheim 1989.
33 J.R. Brisson and J. Carver, *Biochemistry*, 22 (1983) 1362–1368.
34 R.R. Contreras, J.P. Kamerling, J. Breg, and J.F.G. Vliegenthart, *Carbohydr. Res.*, 179 (1988) 411–418.
35 R.P. Veregin, C.A. Fyfe, R.H. Marchessault, and M.G. Taylor, *Carbohydr. Res.*, 160 (1987) 41–56.
36 M.J. Gidley, and S.M. Bociek, *J Am. Chem. Soc.* 110 (1988) 3820–3829.
37 K. Bock, A. Brignole, and B.W. Sigurjskold, *J. Chem. Soc., Perkin Trans. 2*, (1986) 1711–1713.
38 R. Stuike-Prill and B. Meyer, *Eur. J. Biochem.*, 194 (1990) 903–919.
39 B. Meyer, M. Zsiska, and R. Stuike-Prill, in D.P. Landau, K.K. Mon, and H.B. Schuttler (Eds.), *Computer Simulation Studies in Condensed Matters, Physics IV*, Springer, New York, in press.
40 A. Pollex-Krüger, B. Meyer, R. Stuike-Prill, V. Sinnwell, K.L. Matta, and I. Brockhausen, *Glycoconj. J.*, submitted.
41 T. Peters, B. Meyer, R. Stuike-Prill, R. Somorjai, and J.R. Brisson, *Carbohydr. Res.*, in press.
42 S. Levy, W.S. York, R. Stuike-Prill, B. Meyer, and L.A. Staehelin, *Plant J.*, 1 (1991) 195–215.
43 J. Tropp, *J. Chem. Phys.*, 72 (1980) 6035–6043.
44 P.J. Archbald, M.D. Fenn, and A.B. Roy, *Carbohydr. Res.*, 93 (1981) 177–190.
45 T.E. Bull, *J. Magn. Reson.*, 72 (1987) 397–413.